Graduate Theses and Dissertations   Graduate School

4-11-2007

Novel Polymer-Metal Nanocomposites for Applications in Detection and Sensing

Dayling L. Chaparro
University of South Florida

Follow this and additional works at: http://scholarcommons.usf.edu/etd

Part of the American Studies Commons

Novel Polymer-Metal Nanocomposites for Applications in Detection and Sensing

by

Dayling L. Chaparro

A thesis submitted in partial fulfillment
of the requirements for the degree of
Master of Science in Biomedical Engineering
Department of Chemical Engineering
College of Engineering
University of South Florida

Major Professor: Vinay K. Gupta, Ph.D.
John T. Wolan, Ph.D.
Norma Alcantar, Ph.D.

Date of Approval:
April 11, 2007

Keywords: pnipam, microgels, gold nanoparticles, molecular imprinting, interpenetrated networks

DEDICATION

To my family

ACKNOWLEDGEMENTS

TABLE OF CONTENTS

LIST OF TABLES

NOVEL POLYMER-METAL NANOCOMPOSITES
FOR APPLICATIONS IN DETECTION AND SENSING

Dayling L. Chaparro

ABSTRACT

Detection of trace elements such as organic contaminants, explosive residues, and metal ions is an intellectually challenging task in science and engineering. It is also a topic of increasing importance due to its impact on society and the environment. Designing molecularly imprinted materials is one of the most promising approaches to explore sensing and detection applications. "Stimuli-sensitive" polymer materials are ideal candidates for these imprinted sensors as they are able to respond to changes in their environment and can be tailored by cross-linking the polymer chains. The responses can be amplified and transduced into measurable signals due to macromolecular properties provided by the use of a polymer. The purpose of the research in this project is to combine organic polymers with inorganic constituents to tailor the binding properties and the responses of the composite material for detection of metals ions in aqueous solutions.

The research, here, is based on a thermally responsive polymer such as poly(N-isopropylacrylamide) (PNIPAM), which exhibits a well-known reversible volume phase transition in aqueous media around approximately 32°C. Combining cross-linked microgels formed from PNIPAM and its copolymers with gold nanoparticles (GNP) imparts the composite material with optical properties such as intense visible absorption

due to the unique surface plasmon absorption of these small nanoparticles. The use of copolymers allows incorporation of functional groups, such as carboxylic acid, that are potential sites for binding metal ions. Cross-linking of the metal ion binding polymer imprints the metal ion in the PNIPAM microgel network.

In this research, design of the composite material was investigated using copolymers of NIPAM and acrylic acid (AA), copolymers of NIPAM and glycidyl methacrylate (GMA), and interpenetrating networks of PNIPAM and PAA. A broad spectrum of polymerization conditions were studied such as changes in cross-linking density as well as changes in the synthetic procedure. Techniques such as turbidometry, ultraviolet visible spectroscopy (UV-VIS), transmission electron microscopy (TEM), and dynamic light scattering (DLS) were employed to characterize the microgels as well as their composites with GNP. Preliminary investigation of imprinting the microgels with heavy metal ions such as copper was also performed. The novel polymer-metal nanocomposites explored here will serve as an important contribution for the current ongoing research efforts in designing materials in the nano-scale capable of sensing and detecting metal ions in solution with high selectivity.

CHAPTER ONE: INTRODUCTION, MOTIVATION AND BACKGROUND

The broad aim of this thesis project is to develop a novel polymer-metal nanocomposite that can selectively bind heavy metal ions for applications in detection and sensing. The basis of the novel sensor is a "stimuli-sensitive" material because its intrinsic macromolecular properties allow for amplification of a signal. In this research, we have used a thermally responsive polymer known as poly(N-isopropylacrylamide) or PNIPAM. To exploit the unique optical properties of gold nanoparticles (GNP) in the sensing, we have focused on the development of polymer-metal nanocomposites by combining GNP with cross-linked microgels of PNIPAM and its copolymers. For selective binding of the metal-ion, we have explored molecular imprinting in the PNIPAM microgels.

The following sections provide an introduction to the materials, techniques, and concepts that are integral for the research in this thesis.

1.1   Sensing and Detection Using Smart Polymers: Technical Background

Recent advances in materials science and engineering, and in particular, the control of material properties, have been significant in the development of sensors [1,2]. The area of sensor technology is very broad and no simple classification is completely adequate. However, sensors can be categorized by either their chemical composition or their principle of operation [1-4]. Effects such as thermal, electrical, mechanical, optical,

and molecular interactions can be used for sensing [1-4]. Sensors are widely used in all aspects of everyday life and their industrial applications include areas such as automotive, environment, and biomedicine [2, 3, 5, 6].

The design and development of sensors requires many considerations such as the choice of the sensing element, issues of signal amplification, relay, and measurement as well as suitable packaging of the sensor [1]. The sensing element typically refers to a material that fundamentally interacts with the target analyte and can also serve as a transducer by converting the interaction into a measurable output signal [1, 2]. In this context, "smart materials", which are able to respond to changes in their environment, can be used in chemical sensors wherein a chemical change in the environment is transduced into a signal [2, 3, 5, 7, 8]. One of the limitations in the use of "smart materials" is that the variations in environmental conditions and in analyte concentration need to be large to produce measurable responses [1, 3].

"Stimuli-sensitive" polymers are a promising building block for sensing and detection because their intrinsic macromolecular properties allow for amplification of a signal that results from trace concentrations. The "stimuli-sensitive" material used in this thesis research is a thermally responsive polymer known as poly(N-isopropylacrylamide) or PNIPAM. Since a cross-linked network of a polymer makes the network behave as one giant macromolecule, the research in this project focuses on colloidal, cross-linked microspherical particles of PNIPAM or microgels.

Synthesis of PNIPAM microgels was first reported by Pelton and Chibante in 1986 based on techniques performed by Philip Chibante in 1978 [9, 10]. Figure 1 illustrates a schematic of the reversible volume phase transition exhibited by PNIPAM near its

2

lower consolute temperature (LCST) ~32ºC [10-13]. At temperatures below LCST,

PNIPAM microgels are very hydrophilic, swollen particles. However, upon increasing

the temperature to values above LCST the hydrophilic characteristic is lost. Here the

microgels become hydrophobic and expel water from the cross-linked network as the

chains collapse and tend to a globular shape. Because microgels of PNIPAM can

reversibly respond in water to external stimuli such as temperature, these materials have

been of great interest in applications such as chemical/biological sensors, drug delivery,

biomaterials, drug delivery and chemical/biological separations [5, 9, 13-16].

PNIPAM microgels are nonionic but this property can be modified forming

copolymer or interpenetrated networks with electrolyte materials such as monomer or

polymers of acrylic acid [10, 16-21]. PNIPAM microgels, their copolymer and networks are

typically synthesized by surfactant-free precipitation polymerization at ~70ºC using an

initiator that such as potassium persulfate (KPS) [9-11]. The cross-linking character of the

microgels is achieved by adding a divinyl cross-linker such as methylene-bis-acylamide

(MBA). Figure 2 shows a schematic of procedures followed and ingredients used to

synthesize PNIPAM microgels by precipitation polymerization.

1.2   Composites of Polymeric Microgels and Metallic Gold Nanoparticles

Recently, interest in composite materials consisting of metal nanoparticles and

polymers in the form of microgels or networks has also increased. The addition of metal

nanoparticles with unique properties to a smart polymer leads to reversible manipulation

of these properties and greatly expands the range of material properties [2, 6, 22]. The

properties of the polymer-metal nanocomposites depend on the metal nanoparticle size,

shape and concentration as well as the interaction with the polymer matrix [2, 6, 22].

Nanometer sized, colloidal metal particles are of great interest since they can show size-dependent properties different from those exhibited by the bulk metal [2, 6, 22]. The nanometer range at which these effects most significantly occur is between 1-10nm in diameter [2, 6, 22]. Electronic, optical, catalytic, and thermodynamic properties have been observed to be the most significant size-dependent properties of metal nanoparticles [2, 6, 22]. For gold nanoparticles, the surface plasmon absorption is one of the most attractive of these size-dependent properties because it leads to unique optical properties in the visible spectrum of light. GNP solutions show conspicuous colors in solution because of their characteristic plasmon absorptions [2]. This significant property makes GNP suitable for detection and sensing applications.

There are many synthetic strategies to prepared colloidal gold and some of these can be traced back to the middle ages. However, all of the methods used before the 1990's, produced highly unstable gold nanoparticles (GNP) with wide size distributions [6, 23-27]. In 1994, Brust and Schiffrin demonstrated that uniform size of well dispersed GNP can be afforded by protecting their surfaces with alkanethiol molecules in organic media [23, 24]. This method, which is very popular for producing 2-5nm GNP, involves the reduction of a gold salt by the use of sodium borohydride in the presence of a capping agent. Another common approach utilizes reduction of a gold salt and stabilization in presence of trisodium citrate to produce GNP that are greater than 10nm [28, 29].

Several approaches have been developed to prepare polymer-metal nanocomposites in solution. These include combination of the nanoparticle with the polymer by simple diffusion mechanism, functionalization of the nanoparticle and/or

polymer matrix to induce loading, in-situ reduction of metal nanoparticles in the polymer matrix, in-situ synthesis of polymer matrix in presence of preformed metal nanoparticles, as well as evaporation and sputtering, and the use of fluidized beds [6, 22]. Synthesis of polymer-metal nanocomposites can be very tedious and difficult to achieve due to the great importance of emphasizing the best properties of both material for some applications.

1.3   Molecularly Imprinted Materials

The fundamental basis of most chemical sensors is molecular interactions between a target analyte and a receptor. Improvements in sensor technology are, therefore, heavily dependent on optimizing this interaction and making it selective. Molecular imprinting is one approach that allows this selectivity. Molecular imprinting is a new and attractive technique inspired by Fischer's lock-and-key metaphor proposed in 1984 and is considered to be one of the keys for future science and technology in the development of molecular assemblies for molecular recognition applications [7]. In recent years, extension of molecular imprinting to soft materials such as polymers has been actively investigated because of the flexibility in imprinting using chemical cross-linking of the polymer [7, 8, 30].

The concept of molecular imprinting in polymers is based on the complementary polymerization and immobilization (locking) of a template or substrate molecule normally in a porous polymer matrix [7]. The template is first allowed to interact/bind with one of more functional monomers in the matrix in an orderly assembly. Immobilization or locking of these interactions forms cavities that serve as recognition sites

5

complementary and selective for the template molecule. The rebinding process of the substrate relies on its diffusion to the recognition sites through the porous polymer matrix. In principle, many molecules, ranging from small ones such as drugs, hormones, metal ions to large ones such as proteins, could be molecularly imprinted [7, 8, 30]. Several factors influence the preparation of a molecularly imprinted polymer, of which the most important is the selection of the template molecule [7, 8, 30]. Others include the type and availability of functional monomers to bind the template molecule, structure, size and solubility of template, and the application of the resultant imprinted material [7, 8, 30].

For molecularly imprinted polymers (MIP), the imprinting method could be of two types: covalent or non-covalent [30]. For the covalent MIP the polymerization should be carried out under conditions not altering the covalent linkage with the template. Upon rebinding the template in the imprinted polymer it is expected that the covalent linkage is formed [30]. Non-covalent (hydrogen bonding, electrostatic interaction, and coordination-bond formation) functional monomer-template connections, could be obtained in-situ by adding the components to the reaction mixture and removing the template after polymerization with a polar solvent [7, 8, 30]. Synthesis of non-covalent imprinting is easier to achieve, the template is removed easily from the polymer and rebinding and release interactions are faster [7, 8, 30]. On the other hand, covalent imprinting results in the imprinting of more accurate structure of guest-binding site and a wide variety of polymerization conditions can be used [7, 8, 30].

Design of MIPs with improved recognition sites is still a challenge since synthetic techniques are relatively simple and limited when compared to biological systems [7, 8, 30].

MIPs have a many potential application including sensors devices where the MIP serves a recognition element.

1.4   Project Description

This thesis project aims to develop novel polymer-metal nanocomposites with receptor sites that can selectively bind heavy metal ions for applications such as environmental sensing. The use of copolymers of NIPAM and acrylic acid or interpenetrated networks of poly(acrylic acid) with PNIPAM microgels was investigated to incorporate carboxylic acid groups for potential binding of metal ions. Use of the imprinting technique was explored to memorize the shape and binding of the metal ion within the polymeric matrix. Development of the polymer-metal nanocomposite was achieved by combining microgels based on PNIPAM with gold nanoparticles (GNP). Figure 3 shows a simplified schematic of how this procedure was performed. The mechanism followed for the imprinting technique and the expected responses of the composite upon molecular recognition of the target analyte are schematically illustrated in Figure 4. GNP in the composite microgel was used to enhance the optical properties of the composite and allow for colorimetric sensing and detection by transducing the molecular recognition into changes in surface plasmon absorption of the system.

The following chapters provide detailed information on the research performed in this thesis project. Chapter 2 discusses the synthesis and characterization of PNIPAM microgels as well as microgels based on copolymers and interpenetrating networks. Chapter 3 describes several strategies for the preparation of nanocomposites based on microgels and GNP. Molecular imprinting procedures on interpenetrating type of

microgels are summarized in Chapter 4. Finally, Chapter 5 provides a summary of the

research and includes recommendations on modifications and improvements of the

polymer-metal nanocomposites investigated here for applications in detection and

sensing.
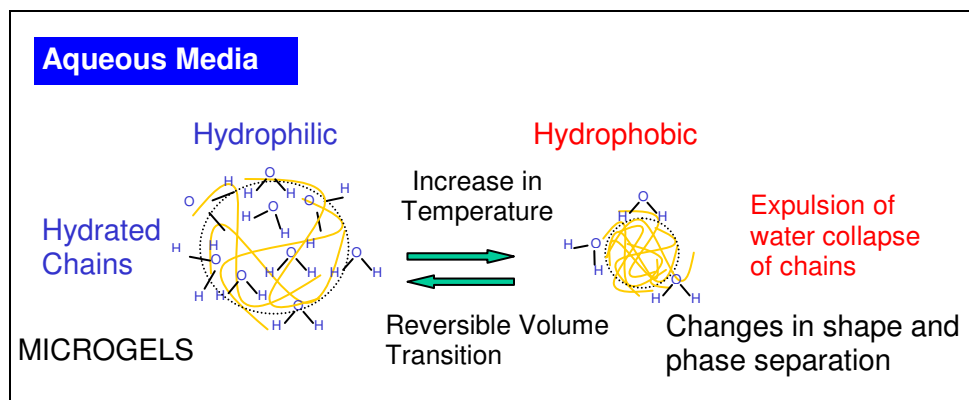
Figure 1: Schematic of the reversible volume phase transition that PNIPAM exhibits due to thermal-stimuli.
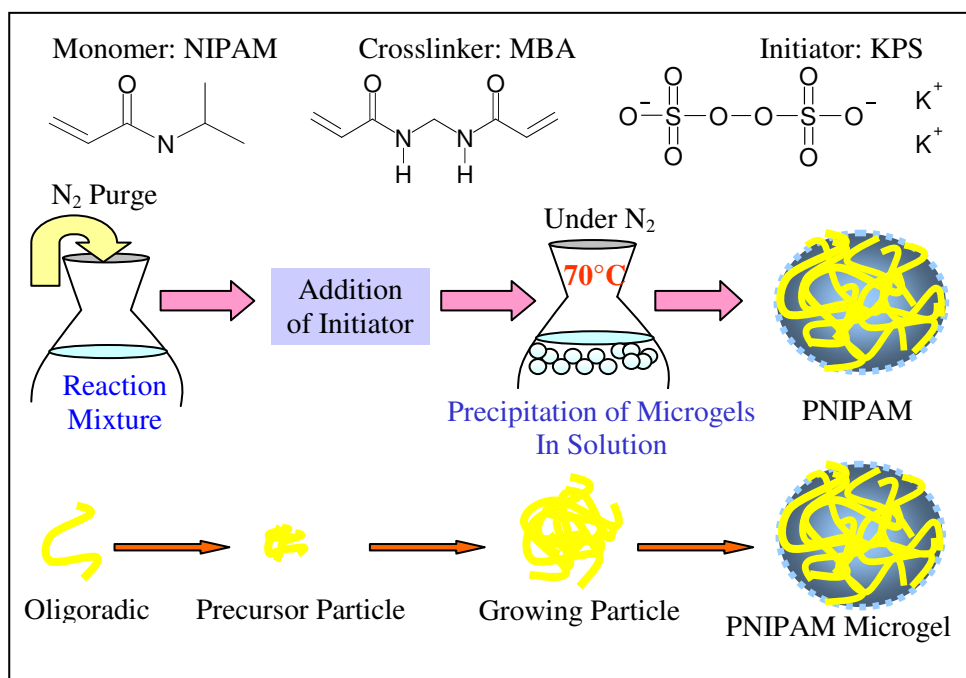
Figure 2: Schematic of synthesis mechanism for the precipitation polymerization of PNIPAM.

-COOH
-COOH
-COOH
-COOH
-COOH -COOH
-COOH
-COOH
-COOH
-COOH
-COOH
-COOH

GOLD NANOPARTICLES

~ 500 nm
PNIPAM MICROGEL WITH
POLY(ACRYLIC ACID) FUNCTIONAL GROUPS

-COOH
-COOH
-COOH
-COOH
-COOH -COOH
-COOH
-COOH -COOH
-COOH
-COOH

NANOCOMPOSITE OF PNIPAM-GNP MICROGELS
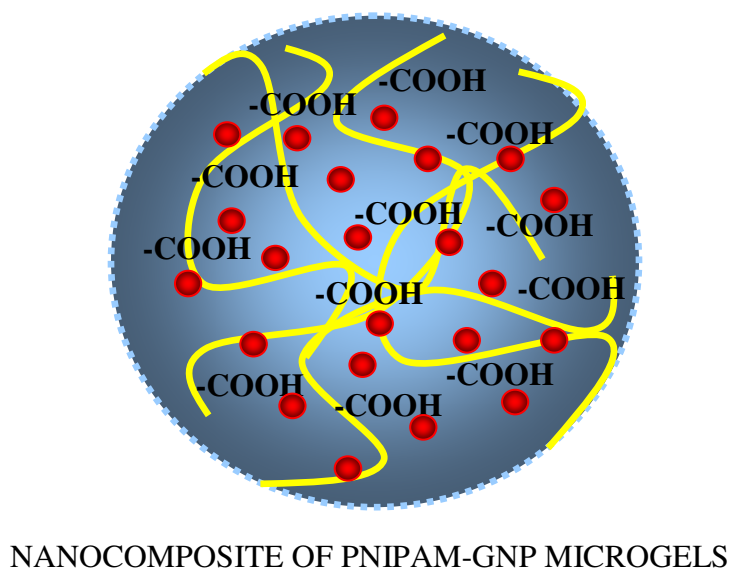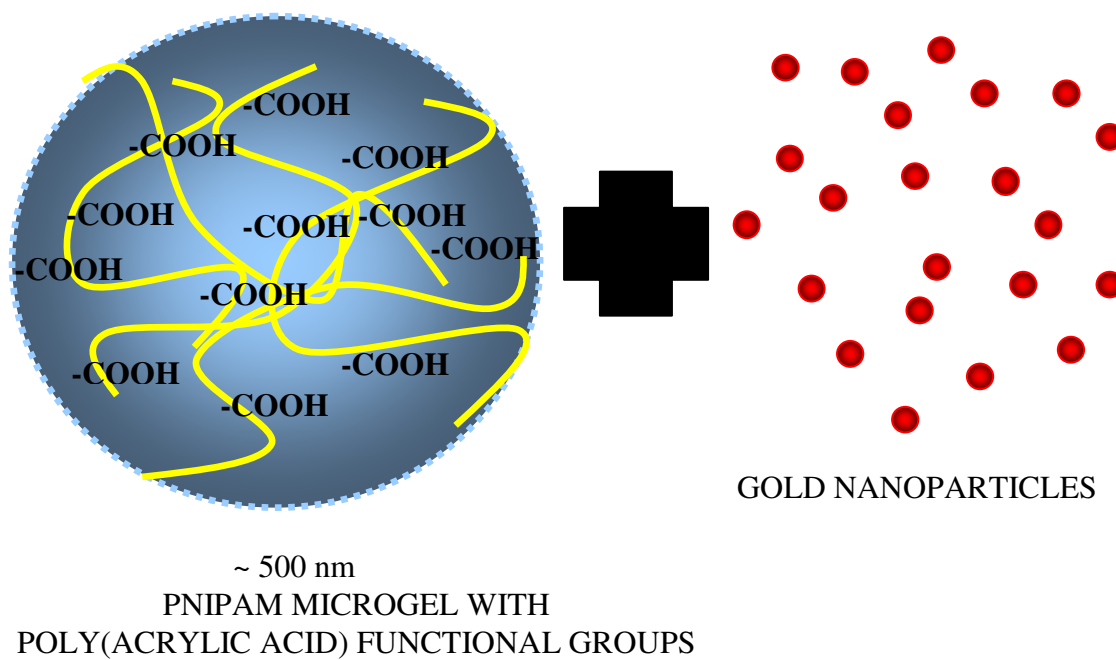
Figure 3: Schematic of the mechanism followed for the preparation of PNIPAM-GNP nanocomposite.

Formation of carboxyl-metal ion complex upon incubation metal ion in composite

Imprinting of metal ion in binding site provided by carboxyls

Complementary shape of metal memorized in the polymeric matrix

Sudden recognition of analyte metal ion induces volume response

Inter-particle distance of GNP changes and the plasmon absorption shifts

Expectation that this change will be most sensitive in the transition region

Figure 4: Schematic of the mechanism followed for the imprinting of metal ion in PNIPAM-GNP nanocomposite.

CHAPTER TWO: SYNTHESIS AND CHARACTERIZATION OF MICROGELS OF THERMALLY-RESPONSIVE POLYMERS

2.1   PNIPAM Microgels

The initial phase of the project focused on preparation of PNIPAM microgels to understand the impact of polymerization conditions. Towards this goal, effects of changes in amounts of monomer, solvent, cross-linker, and initiator were studied. Two microgel samples were prepared of 2 and 4% cross-linking. The cross-linking density was varied since it could be related to the pores size within the microgels and is important in the preparation of composites composed of PNIPAM and small nanoparticles [9, 31-33]. The cross-linking density also affects the response of the microgels - low cross-linking density makes the microgels more flexible when compared to higher cross-linking [9, 31-35].

2.1.1   Experimental Section

Materials

N-Isopropylacrylamide, 97% (NIPAM) was purchased from Aldrich Chemicals (WI) and purified by recrystallization from hexane. N,N'Methyline-Bis-Acrylamide (MBA) and Potassium Persulfate (KPS) were purchased from Aldrich Chemicals (WI) and used without further purification. The hexane used for purification of NIPAM was of reagent grade. Unless otherwise specified, the water used in all synthesis was purified using an EasyPure[TM] UV system (Barnstead, IA).

Synthesis of PNIPAM Microgels

PNIPAM microgels were prepared by precipitation polymerization by using NIPAM monomer, cross-linker and a radical initiator in aqueous media. A fixed amount of recrystallized NIPAM monomer was dissolved in deionized water inside a three neck round bottom flask. A corresponding amount of MBA (cross-linker) was added to the aqueous solution and stirred. A separate solution of KPS (initiator) was prepared by dissolving KPS in 10mL of deionized water. The amount of reactants and solvent for preparation of different samples is summarized in Table 1.

Table 1: Formulation used for PNIPAM microgels.

SAMPLE	NIPAM (mg)	MBA (mg)	KPS (mg)	H_2O (ml)
PNIPAM-2%	300	6	10	30
PNIPAM-4%-I	250	14	20	50
PNIPAM-4%-II	400	22	20	150

The stirred reaction mixture and the KPS solution were bubbled with nitrogen for 30-35 minutes. After bubbling with nitrogen, the reaction mixture was heated up to ~70ºC in an oil bath under a nitrogen atmosphere. The initiator solution was added to the reaction mixture in one shot once the reaction temperature was stable. The reaction was allowed to proceed under nitrogen atmosphere and continuous stirring at ~70ºC for four hours. The resultant milky white microgel solution was cooled down to room temperature and purified. Typically, microgels were purified by centrifugation at 8500 rpm for 30 minutes and redispersing in deionized water. The process was repeated at least four

times. For dry samples, the PNIPAM microgels were dried overnight under vacuum using a vacuum oven at 30-40ºC.

Characterization

In addition to turbidometry, two methods were commonly used to characterize PNIPAM microgels: Transmission electron microscopy (TEM) and Dynamic Light Scattering (DLS). DLS was useful to characterize the particle size and its distribution while TEM was used to probe the shape of the microgels.

TEM characterization in this thesis was performed using a FEI Morgagni 268D instrument. For the analysis of PNIPAM-4% microgels, a drop of an aqueous solution containing the microgels was first placed on a Formvar-coated Cu grid. The excess of sample in the mesh grid was wiped off with a Kim-wipe after ~10 seconds. After allowing the sample to dry for ~1min, the grid was placed in the microscope.

DLS, also know as photon correlation spectroscopy (PCS) and quasi-elastic light scattering (QELS) is a techniques to measure the size of colloidal particles [36]. It measures the size by relating it to the Brownian motion of the particles. A laser light incident on the sample is scattered due to Brownian motion of the particles [36, 37]. In DLS, the intensity of scattered light is measured as a function of time and can be related to the translational diffusion coefficient, which can be converted into a particle size using the Stokes-Einstein equation [36]. The hydrodynamic diameter given by DLS corresponds to that of a sphere that has the same translational diffusion coefficient as the particle [36]. DLS measurements are sensitive to temperature, viscosity, density, and ionic concentration [36]. DLS measurements for this thesis were performed using a Malvern Zetasizer Nano-S instrument. For characterization of PNIPAM-4% microgels, 1mL of diluted aqueous

solution in a cuvette was used. To obtain the changes in the size of PNIPAM microgel

with temperature, the measurements were performed from 24-40ºC.

2.1.2   Results and Discussions

Thermal behavior and volume phase changes of PNIPAM-2% were characterized

by the use of a turbidometer. As shown in Figure 5, the turbidity of the solution increased

during heating and decreased as it was cooled down. Changes in turbidity are an

indication of the shrunken or swollen state of the microgels in solution. As seen in Figure

2.1, the solution became noticeably turbid when temperature reached 30ºC. A steep

turbidity increase was observed up to 40ºC, where turbidity reached a constant value.

The range from 30-34ºC was the volume phase transition (VPT) of the microgels where

the microgels showed a significant change in volume by shrinking or swelling. The mid-

point of this range ~32ºC can be used as a rough transition temperature. A small

hysteresis in the transition phase was observed. However, the transition was reversible

and the solution returned to a transparent state after cooling down.

DLS characterization of PNIPAM-4%-I, shown in Figure 6, illustrates how the

mean size of the microgels decreases upon heating the solution from 24-38ºC. The mean

size of the microgels changed from ~1μm to 500nm. The volume phase transition region

was observed to be from 31-36ºC and the mid-temperature was 33.6ºC. DLS of

PNIPAM-4%-II, in contrast to PNIPAM-4%-I, showed a smaller hydrodynamic diameter

(Figure 7). The size was calculated to be 550nm and 250nm, at a swollen and shrunken

state, respectively. The smaller size of PNIPAM-4%-II was attributed to polymerization

with three times more solvent. PNIPAM-4%-II also showed a smoother size trend which

is characteristic of a smaller polydispersity. Therefore, it is expected that these particles are more uniform in size and better dispersed in solution than PNIPAM-4%-I.

The changes in appearance of PNIPAM microgels in solution due to thermal responses can be seen in Figure 8. The three pictures of a solution containing PNIPAM microgels illustrate the gradual change increase in turbidity as the solution is heated to its transition temperature. The solution is transparent at temperatures below LCST and as the temperature reaches the LCST the solution starts becoming turbid. The PNIPAM solution changes from transparent to turbid or milky-white when the mean size of the microgels decreases and the refractive index contrast becomes large between the particles and the solvent. As seen in the TEM image shown in Figure 9, the size of the microgels was observed to be ~440nm at a shrunken state, which agrees with DLS characterization at temperatures above LCST.

In summary, precipitation polymerization is a useful synthetic technique for the preparation of PNIPAM microgels. The amount of cross-linker could be varied without changing the thermal behavior and VPT dramatically to trigger different states of densities in the microgels. This, in fact, could serve to indirectly control the pore size and flexibility of the polymer and potentially form composites by loading and retaining nanoparticles within the microgel network [33]. The amount of solvent is an important material to synthesize monodisperse microgels of different sizes. It is known that combination with surfactants such SDS (sodium dodecyl sulfate) in 1 mole%, can lead to the formation of microgels of even 100nm in diameter [11, 16, 33, 38].

2.2   Microgels Formed from Copolymers of P(NIPAM-AA)

Copolymers of P(NIPAM-AA) microgels were prepared with the purpose of obtaining a material with functional groups capable of binding metal ions and metal nanoparticles while keeping the unique thermal-responsive properties of NIPAM. The functional groups provided by acrylic acid (AA) are carboxylic acid groups (COOH). These not only have the potential to bind metal cations such as copper but also to modify physical properties of the microgels [16, 20, 38]. When present in the microgels, COOH groups increase hydrophilic characteristics, which affect the transition temperature of the microgel and leads to a higher LCST [16, 20, 38]. Experiments described in this section were designed to understand the effects of acrylic acid monomer concentration on P(NIPAM-AA) copolymer microgels and the changes in their VPT temperature.

2.2.1   Experimental Section

Acrylic acid 99% and hydroxyl-ethyl-acrylate (HEA) 96%, were both purchased from Aldrich Chemicals (WI) and used without further purification. The synthetic procedures and characterization techniques used for P(NIPAM-AA) microgels were similar to the ones discussed in section 2.1.1. Precipitation polymerization was carried in deionized water and initiated by KPS. Modifications to the procedure were mainly in the addition of AA and HEA monomers to the reaction mixture along with NIPAM and MBA prior initiating the reaction according to the amounts shown in Table 2. Two copolymers of P(NIPAM-AA) cross-linked with MBA were prepared: P(NIPAM-AA)-5% and P(NIPAM-AA)-25%. The percentage in the above naming designates the mole % of AA monomer used relative to NIPAM for the preparation of the copolymer.

Table 2: Formulation used for P(NIPAM-AA) microgels.

SAMPLE	NIPAM (mg)	AA (mg)	HEA (mg)	MBA (mg)	KPS (mg)	H₂O (ml)
P(NIPAM-AA)-5%	300	10	6	16	10	30
P(NIPAM-AA)-25%	300	46	14	17	11	30

2.2.2 Results and Discussions

Turbidity measurements were used to characterize the thermal behavior and VPT of the P(NIPAM-AA) copolymer microgels. Figures 10 and 11, illustrate the turbidity data of P(NIPAM-AA)-5% and P(NIPAM-AA)-25%, respectively. P(NIPAM-AA)-5% exhibited a transition region from ~33-36ºC and a mid temperature of ~34ºC. As expected, copolymer microgels containing AA exhibited a slightly higher LCST in comparison to PNIPAM microgels due to the presence of COOH in their networks. P(NIPAM-AA)-25% showed a similar thermal-behavior and VPT to P(NIPAM-AA)-5% even though their AA molar percentage differed by 20%. This effect was attributed to the increase of HEA composition in the preparation of the copolymer with 25 mole % AA. HEA increases size of porous voids and is favorable for making composites [16, 20, 39]. However, it also enhances the hydrophobic forces in the microgels. Therefore, the thermal-behavior and changes in VPT induced by an increase in AA composition are inhibited to some extent by an increase in HEA composition in the synthesis of these copolymers.

In summary, precipitation polymerization is also useful for synthesizing copolymers of PNIPAM microgels. The composition of AA can be varied to control COOH groups within the microgels as well as their hydrophilic forces and VPT.

Hydrophobic monomers such as HEA counteract the interactions of AA and prevent the LCST from increasing to high values in copolymers of PNIPAM and AA.

2.3   Microgels Formed from Copolymers of P(NIPAM-GMA)

In this section, thermo-responsive polymer particles were synthesized using a combination of Glycidyl methacrylate (GMA) and NIPAM monomers following a procedure similar to those reported by Kawaguchi [40-42]. GMA introduces epoxy groups in the microgel that can serve as reactive sites for immobilization of functional groups, such as amine (-NH) and thiol (-SH), that can further be used to hold gold nanoparticles in the microgel network using chemical interactions [40-42].

2.3.1   Experimental Section

Glycidyl methacrylate (GMA) stabilized 97%, was purchased from Acros Organics (NJ) and used after purification from inhibitors with neutral alumina by column chromatography. P(NIPAM-GMA) copolymer microgels were also prepared by precipitation polymerization using similar procedures explained in detail in section 2.1.1 and according to values in Table 3. However, since GMA is a hydrophobic monomer that gets consumed faster than NIPAM, some reaction conditions were adjusted to favor the synthesis of a more uniform copolymer in terms of monomer compositions [40-42]. To bring the reaction rate of these two monomers to an approximate value, the temperature at which the polymerization was carried out was increased to 80ºC and the reaction time extended to six hours. Purified GMA monomer was added to an aqueous solution containing NIPAM and MBA prior initiating the reaction. The reaction was initiated as

before by adding KPS. The resultant copolymer was purified by centrifugation as explained in section 2.1.1.

Table 3: Formulation used for P(NIPAM-GMA) microgels.

SAMPLE	NIPAM (mg)	GMA (mg)	MBA (mg)	KPS (mg)	H$_2$O (ml)
P(NIPAM-GMA)	673	423	7	64	100

2.3.2 Results and Discussions

P(NIPAM-GMA) copolymer microgels were characterized by DLS. Figure 12 shows the hydrodynamic diameter of the microgels at a swollen and shrunken state was 450nm and 250nm, respectively. The transition region of the microgels ranged from 30-35ºC. As expected, the thermal behavior and VPT was similar to that observed on PNIPAM and P(NIPAM-AA) microgels. However, the presence of GMA made the microgel solution looked opaque at ambient temperature. As a result, the jump in turbidity due to heating above LCST is not as significant as observed for PNIPAM microgels in Figure 7.

2.4 Microgel of PNIPAM with Interpenetrating Networks of PAA

Interpenetrated networks (IPNs) of PNIPAM and AA were synthesized in this section by two methods-a two-step approach and a one-step method [15, 18, 19, 21]. These were prepared with the purpose of obtaining a thermo-responsive material having as many carboxylic acid groups as possible within the microgel. According to literature, the hydrophilic PAA components in a IPN-type case are not chemically attached to the

PNIPAM network [19, 43-45]. Therefore, they should not alter the LCST of the PNIPAM

microgels and their behavior. The IPN-type material will be investigated for their

potential application in the preparation of nanocomposites and molecularly imprinted

PNIPAM microgels.

2.4.1 Experimental Section

A sodium salt of PAA (Typical Mw 15,000) and N,N,N^1N^0–

tetramethylethylenediamine, 99% reagent (TEMED) were both purchased from Aldrich

Chemicals (WI) and used without further purification.

Synthesis of Microgels of PNIPAM with Interpenetrating Networks of PAA

One-Step Approach: PAA was mixed together with NIPAM and MBA according to

Table 4. Following precipitation polymerization procedures explained in section 2.1.1,

the reaction was carried out under a nitrogen atmosphere and continuous stirring at ~70ºC

for four an a half hours. The pH value of the reaction mixture was measured to be ~9.0

before addition of the initiator. The product, PNIPAM/PAA-IPN-I, was purified and

characterized in a similar manner as in previous sections.

Table 4: Formulation used for PNIPAM/PAA-IPN-I microgels.

SAMPLE	NIPAM (mg)	PAA (ml)	MBA (mg)	KPS (mg)	H_2O (ml)
PNIPAM/PAA-IPN-I	2000	3	80	40	400

Two-Step Approach: PNIPAM microgels were first prepared using procedures outlined in

section 2.1.1. These microgels were mixed with AA in cold DI water. The round bottom

flask containing the reaction mixture was placed in an ice bath to lower the solution's

temperature to ~ -5ºC. This temperature was used to keep the microgels in a swollen state

while polymerization of AA to PAA chains takes place within the PNIPAM networks.

TEMED was used to accelerate the polymerization kinetics at -5 ºC. Table 5 provides the

amounts of the reagents used. The reaction proceeded under a nitrogen atmosphere and

continuous stirring for six hours. The product, PNIPAM/PAA-IPN-II, was purified four

times by centrifugation, characterized and stored for further use.

Table 5: Formulation used for PNIPAM/PAA-IPN-II microgels.

SAMPLE	PNIPAM-4%-II (mg)	AA (mg)	KPS (mg)	TEMED (ml)	H_2O (ml)
PNIPAM/PAA-IPN-II	100	300	6	0.06	100

2.4.2   Results and Discussions

PNIPAM/PAA-IPN-II was characterized by DLS as shown in Figure 13 The VPT

of this IPN was similar to that observed for its seed, PNIPAM-4%-II. However, the

hydrodynamic diameter in the swollen state was decreased by 50nm when compared to

the swollen diameter of PNIPAM-4%-II. During the preparation of PNIPAM/PAA-IPN-

II no cross-linker (MBA) was used to in the polymerization of AA. However, unreacted

vinyl groups within PNIPAM-4%-II can undergo cross-linking with some of the PAA

chains and this cross-linking of PAA chains within the microgel can prevent the IPN

microgel from swelling to the same extent as the pure PNIPAM microgel. The

composition of AA was found to be 48% by mass (*measurements of total nitrogen

content for estimation of AA content were done by Mr. Cecil Coutinho).

DLS characterization of PNIPAM/PAA-IPN-I is illustrated in Figure 14. The size at the swollen state was ~300nm more than that of PNIPAM/PAA-IPN-II and the size ranged from ~800-450nm. The composition of AA was 52% by mass, which is closed to that obtained for PNIPAM/PAA-IPN-II. Thus, both one-step and two-step procedures proved to be useful in the preparation of PNIPAM microgels with enough AA content. However, the one-step approach was found to be simpler and more controllable than the one used to synthesize PNIPAM/PAA-IPN-II.
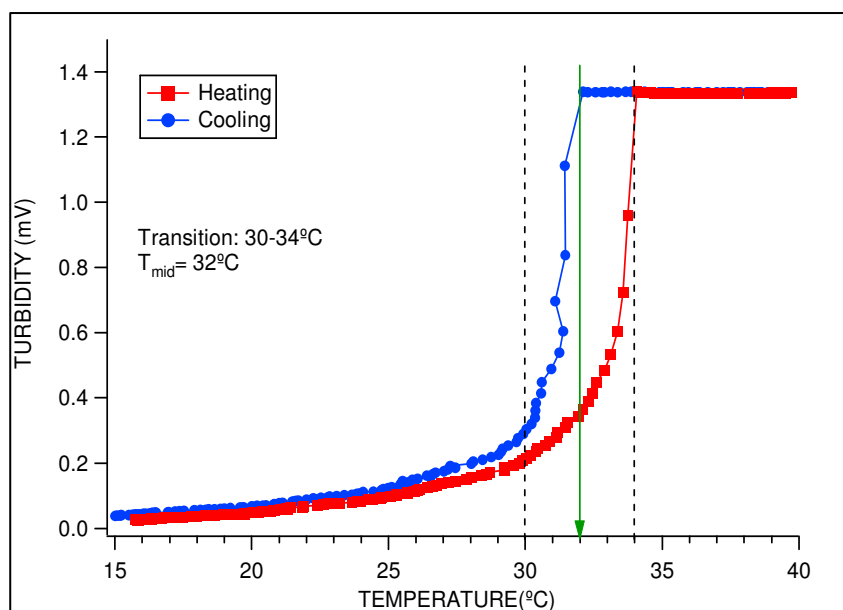
Figure 5: Turbidity data of PNIPAM-2%.
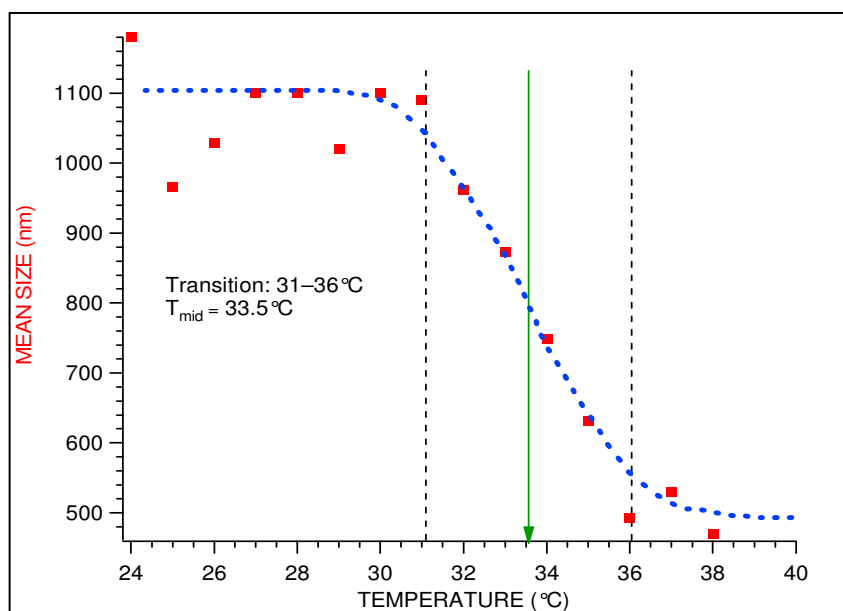
Figure 6: DLS of PNIPAM-4%-I. Lines are drawn as a guide.
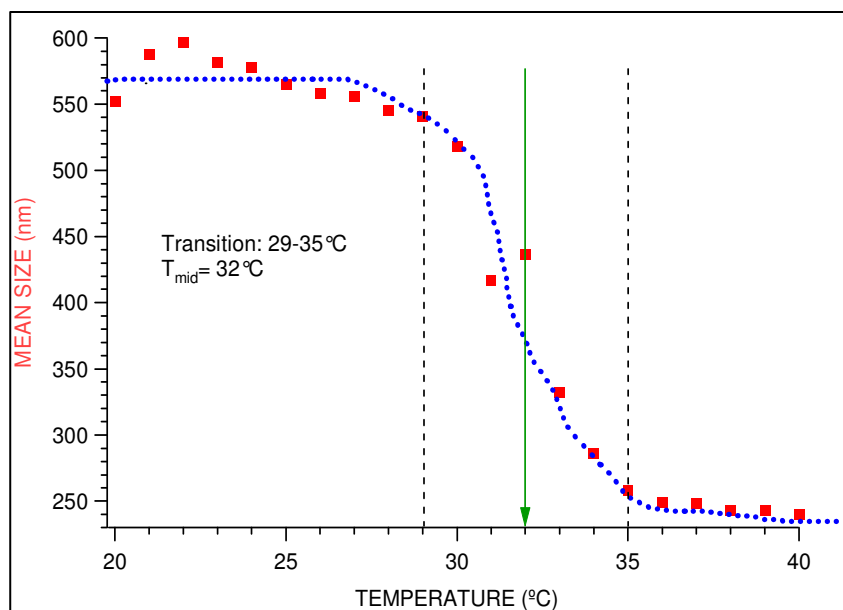
Figure 7: Mean size of PNIPAM-4%-II. Lines are drawn as a guide.

Figure 8: Changes in appearance of PNIPAM microgels upon heating the solution.

Figure 9: TEM of PNIPAM-4%-I.

Figure 10: Turbidity data of P(NIPAM-AA)-5%.

Figure 11: Turbidity data of P(NIPAM-AA)-25%.

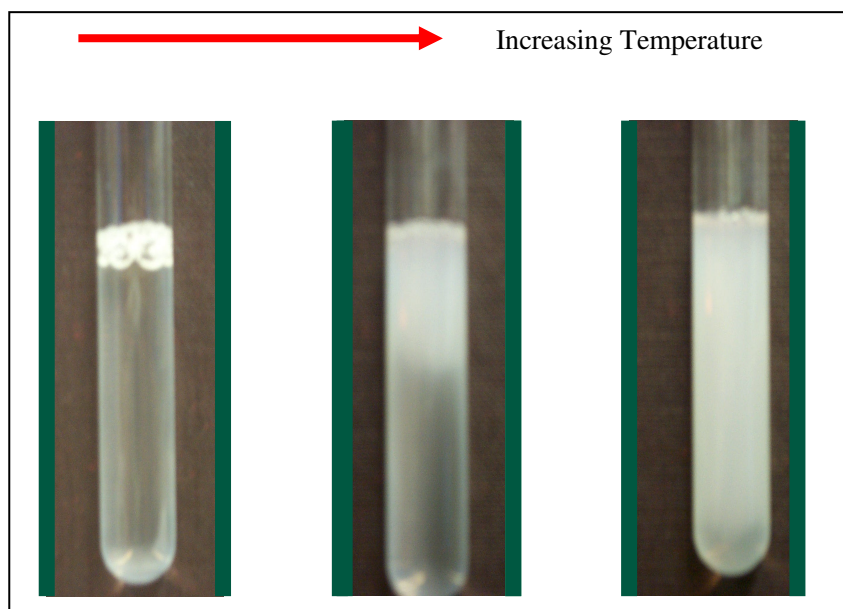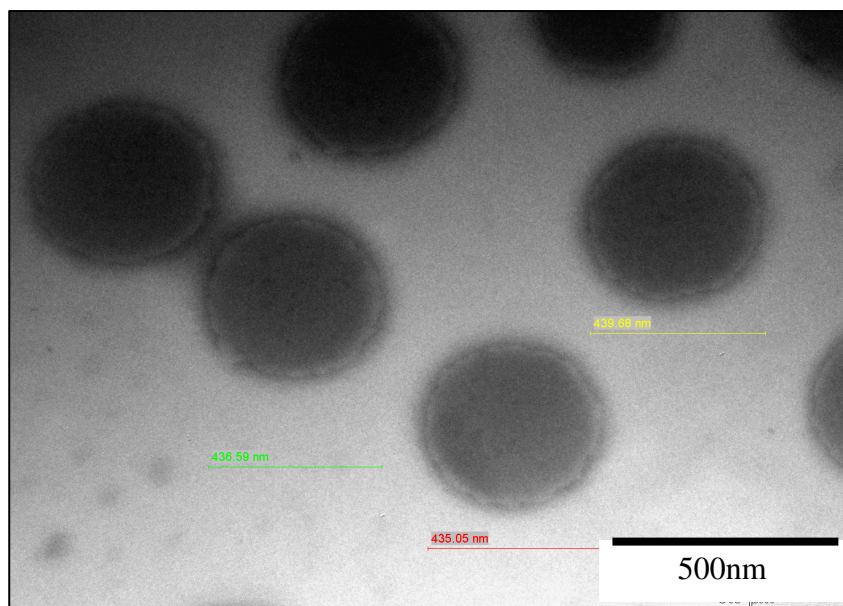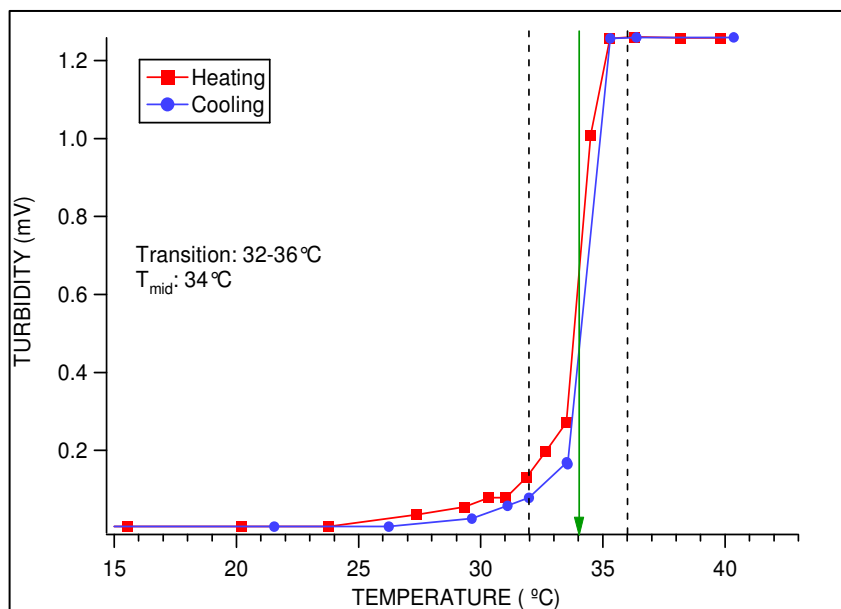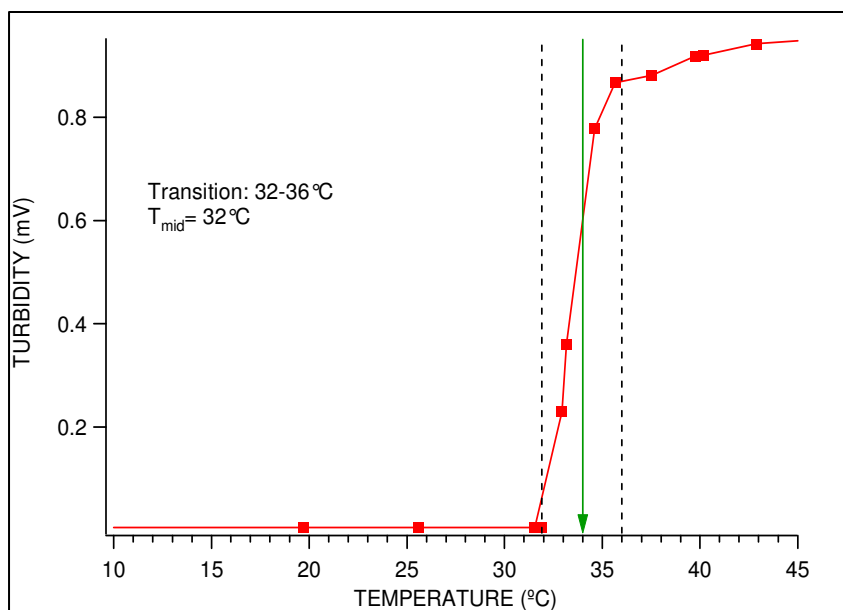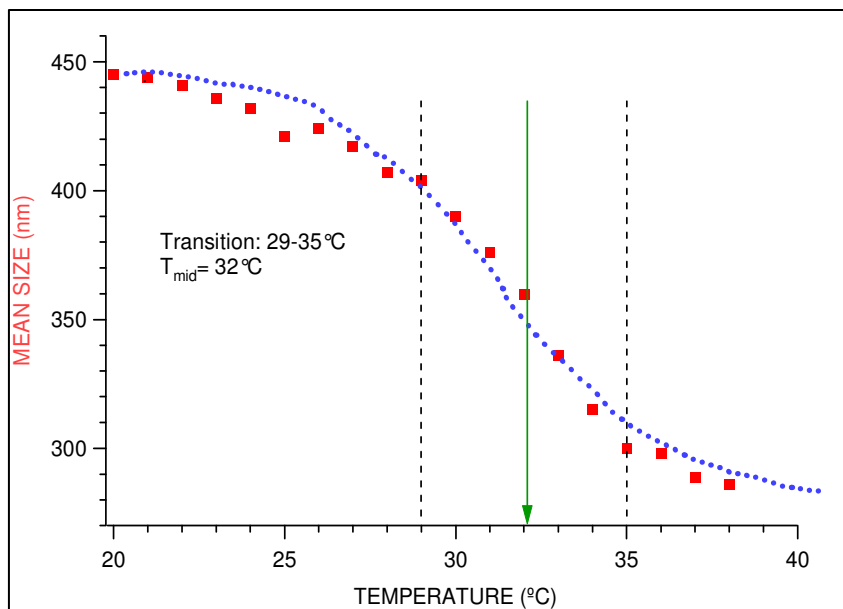**Figure 12: DLS of P(NIPAM-GMA). Lines are drawn as a guide.**
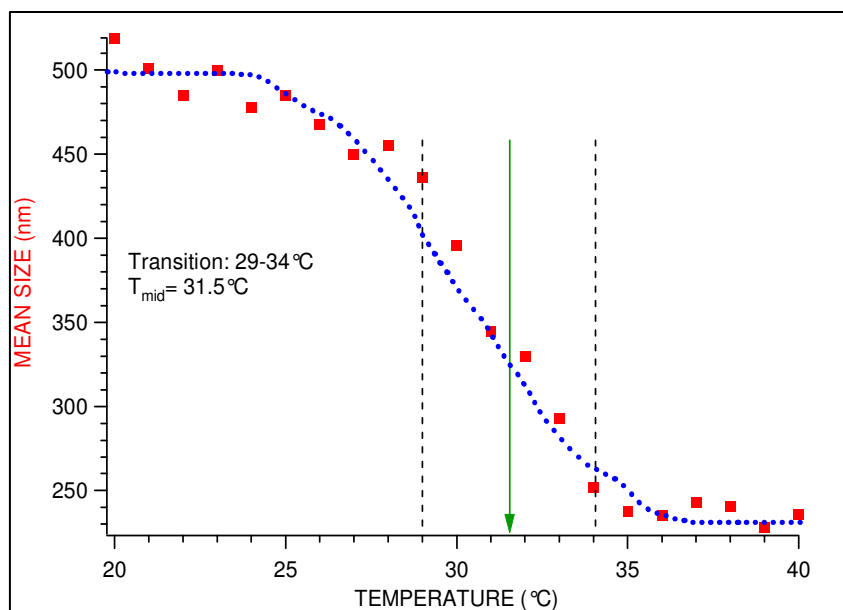
Figure 13: DLS of PNIPAM/PAA-IPN-II. Lines are drawn as a guide.
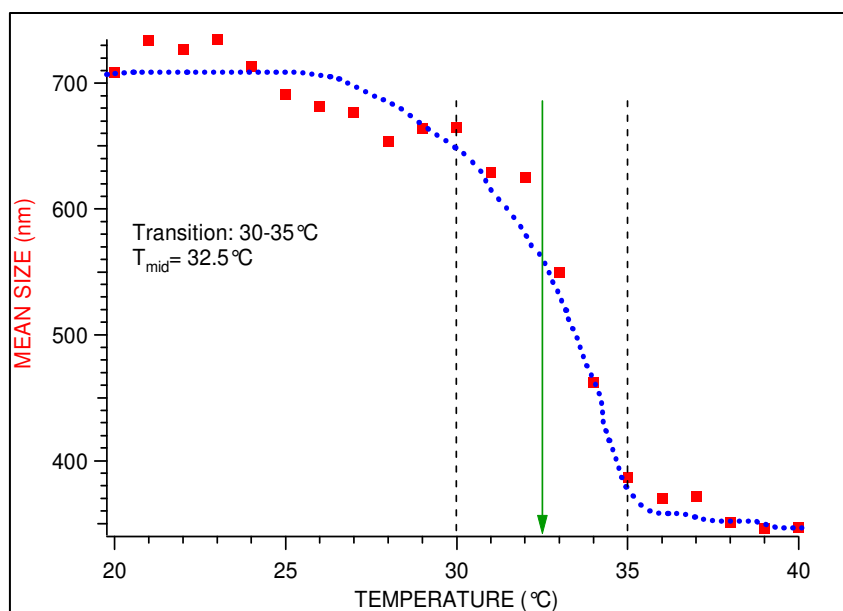
Figure 14: DLS of PNIPAM/PAA-IPN-I. Lines are drawn as a guide.

CHAPTER THREE: POLYMER-METAL NANOCOMPOSITES OF MICROGELS AND GOLD NANOPARTICLES

3.1 Nanocomposites Based on PNIPAM Microgels and Gold Nanoparticles

In this section the preparation of nanocomposites based on mixing PNIPAM microgels and GNP is explored. This method was selected over others because it is simple to perform. The approach was based on physical entrapment of GNP by diffusion through the pores of PNIPAM microgels. The diffusion process was achieved by means of the stimuli-responsive reversible behavior of PNIPAM. Citrate-stabilized GNP of ~12nm in size and PNIPAM-2% (*cf* Section 2.1) were the main components used for the preparation of the nanocomposite.

3.1.1 Experimental Section

Citrate-stabilized GNP (JYS-I-1-1P) were synthesized by Dr. J-Y Shim using procedures reported in literature [29, 46, 47]. The nanocomposites based on PNIPAM-2% and citrate-stabilized GNP was prepared by a simple diffusion mechanism. The microgels were swollen and shrunken by altering the solution's temperature below and above LCST to facilitate the diffusion of GNP through their pores.

A 1mg/ml aqueous solution of PNIPAM-2% was mixed together with JYS-I-1-1P citrate GNP (~12nm) in a volume ratio of the microgel to GNP dispersion of 2:3. The solution was gently shaken for a few seconds, placed in an ice bath and stirred for 1 hour. The vial containing the resulting solution of PNIPAM-2%-Citrate-GNP was transferred

29

to an oil bath at 40ºC and stirred at same rate as before for an additional hour. The two

steps of heating and cooling mentioned above constitute one cycle. The sample was

subjected to three cycles over 6 hours. The nanocomposite sample was characterized and

stored in the refrigerator for further use.

In addition to techniques used in Chapter 2, UV-VIS spectroscopy was utilized to

measure the light absorption of GNP and nanocomposites composed of microgels. UV-

VIS spectroscopy characterization equipments used here were: Jasco Spectrophotometer

(Model V-530) and Ocean Optics USB-2000 Model.

3.1.2   Results and Discussions

Turbidometry showed that the LCST for the nanocomposite was near 33ºC. In

comparison to the PNIPAM-2% the VPT of the composite was narrower and significantly

more discontinuous (Figure 15). The resultant nanocomposite solution was pink at

temperatures below LCST (Figure 16). The pink appearance of the solution was due to

the surface plasmon absorbance of the GNP. However, upon heating above LCST the

turbidity of the polymer dominates the appearance.

When the composite was purified by centrifugation to separate PNIPAM-2%-

Citrate-GNP from GNP that was outside the microgels, a dark colored precipitate was

obtained. This precipitate was re-dispersed in water. TEM images revealed that formation

of the composite was not achieved using a simple heating and cooling cycle in our

samples. Figure 17 (A) shows TEM of citrate-stabilized GNP and (B) shows the

"composite" sample. An examination of the TEM reveals that the citrate-GNP was

randomly dispersed throughout the sample and did not show any visible signs of

entrapment within the spherical microgels (note: the lightly cross-linked microgels are not clearly observed in the image because they only weakly scatter the electrons in TEM).

Failure to entrap GNP can be attributed to possible separation of GNP from the microgel network upon purification due to large pore size and poor stability of GNP within the network. Minimization of the pore size of PNIPAM microgels is achievable by increasing cross-linking density and incorporation of functional groups in the microgel or on the surface of the GNP can help stabilize the GNP within the microgel.

3.2   Nanocomposites Based on P(NIPAM-AA) Copolymer Microgels

Since results from section 3.1 suggest that functional groups that interact chemically with GNP can be useful to form nanocomposites, we used P(NIPMA-AA) copolymer microgels that incorporated thiol (SH) groups. Thiol groups have affinity to both Au^{3+} ions and colloidal gold [48, 49]. By incorporating thiol groups our goal was to stabilize GNP within P(NIPAM-AA) copolymer microgels. The COOH groups from the acrylic acid could then be expected to bind metal ions and form a complex that could be used to prepare an imprinted polymer.

The approach used to introduce thiols groups in P(NIPAM-AA) copolymer microgels was to combine two type of cross-linkers during the polymerization of NIPAM and AA (*cf* section 2.2). The two chemical cross-linkers used to synthesize the copolymer microgels were MBA and N,N-cystamine-bis-acrylamide (CBA) [48, 49]. Cross-links formed with MBA are chemically stable and inert, and do not have affinity towards gold [48, 49]. CBA is a cross-linker containing reactive disulfide bridges that can form polymer

31

chain transfer agents known as sulfhydryls [48, 49]. In this manner, CBA can take part, not only in the branching of the polymer backbone through thiol-ethers bonds, but in the chemical stabilization of GNP within the copolymer microgel [48, 49].

In this context, a second approach was also investigated to promote the interaction of GNP with the microgel. GNP was synthesized in an organic medium and transferred to water using a positively-charged ligand known as 4-dimethylaminopyridine (DMAP) [50]. As previously reported, DMAP ligand attaches to the surface of the colloidal gold nanoparticles and stabilizes the GNP in toluene as well as facilitates the phase transfer of GNP from toluene to water [50]. By using DMAP and making the GNP surface positively charged, the expectation was that the deprotonated, negatively charged COOH groups of acrylic acid could influencing the loading of GNP via electrostatic attractions.

3.2.1 Experimental Section

Materials

N,N-cystamine-bis-acrylamide (CBA) was purchased from Sigma-Aldrich Chemicals (WI) and used without further purification. Hydrogen tetrachloroaurate ($HAuCl_4$), tetraoctylammonium bromide (TOAB), sodium borohydride ($NaBH_4$), 4-dimethylaminopyridine (DMAP) and mercapto-undecanoic acid (MUA) were all purchased from Acros Organic (NJ).

Synthesis of P(NIPAM-AA) Copolymer Microgels with CBA Cross-Linker

P(NIPAM-AA) copolymer microgel with a composition of 26 mole% of AA were prepared by precipitation polymerization following similar procedures used to synthesize copolymer microgels of PNIPAM and AA in Chapter 2. Since CBA is not soluble in

water, it was dissolved in 250µL methanol before addition to the reaction mixture. Table 6 gives details on the amount of each reactant used to polymerize the thermo-responsive nanomaterial. The reaction proceeded for 4 hours. The product was purified by dialysis (2 weeks) and centrifugation (twice). The polymer, 260 mg, obtained upon drying it under vacuum was stored in a refrigerator for further use. P(NIPAM-AA) copolymer microgel were characterized by turbidometry, DLS and TEM.

Table 6: Formulation used for P(NIPAM-AA) with CBA cross-linker.

SAMPLE	NIPAM (mg)	AA (mg)	HEA (mg)	CBA (mg)	MBA (mg)	KPS (mg)	H_2O (ml)
P(NIPAM-AA)	304	49	19	8	120	10	30

Synthesis of Gold Nanoparticles Stabilized by DMAP

Gold nanoparticles (GNP) were synthesized in an organic medium by adapting the method reported by Brust *et al* [23, 24]. A 38mM aqueous solution of hydrogen tetrachloroaurate ($HAuCl_4$) was added slowly to a 13mM solution of tetraoctylammonium bromide (TOAB) in toluene. The solution was stirred for 1.5 hr to allow the metal salt to be transferred to the organic phase. To reduce Au^{3+} ions, a freshly prepared aqueous solution of 0.13M sodium borohydride ($NaBH_4$) was added dropwise to the mixture while stirring. The solution turned ruby red after the gold reduction was allowed to stir overnight. The organic layer was separated from the aqueous layer and washed with water, 0.1M HCl, and 0.1M NaOH. The procedure was repeated three times and a final wash with DI water was performed. The organic layer containing the GNP stabilized by TOAB was allowed to dry with anhydrous sodium sulfate ($NaSO_4$) for 1

hour. The TOAB-GNP recovered in 20mL of toluene was transferred to an amber bottle and stored in the refrigerator for characterization and further experiments. TOAB-GNP was characterized by UV-VIS spectroscopy and TEM. For TEM measurements, a drop of the toluene solution containing TOAB-GNP was placed in a Formvar-coated Cu grid. Particle sizing was also performed using DLS.

DMAP-GNP was prepared by typically adding 20mg of solid DMAP to 250μL of the toluene solution containing TOAB-GNP. The displacement of TOAB by DMAP was allowed to proceed for 1 hour without shaking the solution. Displacement of TOAB by DMAP caused GNP to precipitate slowly out of solution. DMAP pellets appearance changed from white to black, suggesting GNP attachment. The supernatant, toluene, was then removed carefully with a glass pipette to separate it from the black DMAP-GNP pellets. The samples were dried with a low flow rate of N_2 to help evaporate the remaining of toluene for 1 hour. The resulting DMAP-GNP were dispersed in water by adding 250μL of DI water to the tube containing the particles. The solution changed from transparent to turbid as dispersion of the particles in water phase was taken place. DMAP-GNP solution (pH 11) was sonicated for 20 minutes to break down aggregates and then characterized by TEM.

Nanocomposites Based on P(NIPAM-AA) Microgel with CBA Cross-linker

To prepare the nanocomposites based on P(NIPAM-AA) copolymer microgel cross-linked with MBA and CBA, a mixing procedure was used. A volume of 0.45mL of positively charged DMAP-GNP solution was added to 0.5mL of 0.2mg/mL of P(NIPAM-AA). The sample was then sonicated, well-shaken, and stored in the refrigerator until further processing. Some sedimentation was observed the next day. After shaking the

34

sample, 0.244mg of MUA (5mM in ethanol) was added to the sample to functionalize the GNP surface already loaded within the microgel.

3.2.2 Results and Discussions

P(NIPAM-AA) microgels with CBA cross-linker showed a reversible volume transition with temperature. As shown in Figure 18, the mean size of the microgels decreased from 1.2μm to 0.450μm upon heating. The solution changed from transparent to milky white as microgels collapsed.

Figure 19 shows that the maximum absorbance peak of TOAB-GNP was at 515nm, which is indicative of well-dispersed GNP in solution. The TEM characterization (Figure 20(B)) shows that the particles ranged in size from 4 to 6 nm, which is consistent with the shape of the spectrum in Figure 19. Figure 20(A) shows the size distribution of the particles using DLS. The mean size of TOAB-GNP was approximately 7 nm in diameter, which agrees well with results shown in Figures 19 and 20(B).

The P(NIPAM-AA)DMAP-GNP composite showed a similar volume transition with temperature (Figure 21) but exhibited a mean size smaller than the microgel in Figure 18. This decrease in size can be attributed to electrostatic effects from the DMPA-GNP within the microgel and different additives such as HCl and DMAP. The visible absorption at 528nm of the composite materials in solution indicated that the GNP was not in a significant aggregated state within the microgels at ambient temperature (Figure 22). The 15nm wavelength difference upon comparison of TOAB-GNP and P(NIPAM-AA)DMAP-GNP spectra (Figures 19 and 22, respectively) was attributed to the phase transfer of GNP from organic to aqueous medium by DMAP ligand.

TEM of P(NIPAM-AA)DMAP-GNP composites showed the presence of GNP inside microgels for the composite system (Figure 23). However, after dialysis for one day it was observed that GNP were not retained within the copolymer microgel. Alternatively, purification via centrifugation led to the nanocomposite becoming adhered to the walls of the centrifuge tube. Literature reports have indicated that a GNP complex stabilized with DMAP and/or MUA in water requires a basic environment [50, 51]. However, redispersion of the nanocomposite in aqueous solution from the centrifuge tube walls was difficult even after raising the pH of the solution. Another drawback of this system was that microgels do not undergo phase transition at basic pH [38].

3.3   Nanocomposites Based on P(NIPAM-GMA) Copolymer Microgels

Since the approach described in section 3.2 using DMAP functionalized GNP did not provide a promising approach to preparing the nanocomposites, an alternative strategy based on P(NIPAM-GMA) copolymer microgels was explored to obtain a more stable composite that could exihibit unique and distinctive properties in response to changes in temperature.

P(NIPAM-GMA) copolymer microgels have epoxy groups that can be used to introduce functional groups such as amine and thiol [40-42]. Amine groups complex with gold ions and can facilitate metal nanoparticles nucleation and growth. However, the method adopted in our studies relied on interactions between negatively-charged GNP to the positive amine groups inside the copolymer microgels. This approach was preferred over the in-situ synthesis of GNP because it is simpler and less intrusive. The in-situ synthesis method can lead to particle aggregation, polydispersity, and nucleation of

particles outside the microgels, which can pose problems because the aggregation state of the colloidal gold influences their optical properties [2, 6].

3.3.1 Experimental Section

Materials

Trisodium citrate (TSC) and cystamine·2HCl was purchased from Sigma Aldrich (WI) and used without further purification.

Synthesis of Gold Nanoparticle Stabilized by Trisodium Citrate

Aqueous solutions of citrate-stabilized GNP (~6 nm) were prepared by reducing Au^{3+} through the use of $NaBH_4$. A 9mL aqueous solution containing 0.250mL of 0.01M of $HAuCl_4$ and 0.500mL of 0.01M TSC was prepared in a scintillation vial. A volume of 0.250mL of ice cold 0.1M $NaBH_4$ freshly prepared was added to the solution in one shot while stirring. Immediately after adding the reducing agent, the solution turned orange indicating the formation of GNP. The GNP solution was stirred for an additional two hours with open top to allow degassing of excess $NaBH_4$ from solution. Particles were characterized by DLS and UV-VIS spectroscopy.

Amino-Functionalized P(NIPAM-GMA)CYS Copolymer Microgels

Amino groups were introduced in P(NIPAM-GMA) copolymer microgels by allowing the epoxy groups in P(NIPAM-GMA) (*cf* Chapter 2.3) to react with thiol groups of cystamine·2HCl. A mixture of 30mg of P(NIPAM-GMA), 100mg of cystamine·2HCl, and 50mL of water was transferred to a scintillation vial. The mixture was stirred at room temperature at a pH value of 11 adjusted with 1M NaOH. The reaction continued for 24 hours. The amino-functionalized copolymer microgels (P(NIPAM-GMA)CYS) were

purified by centrifugation (4 cycles). The yellow-brown precipitate was redispersed in water and purified by 3 days of dialysis.

Nanocomposite Based on P(NIPAM-GMA)CYS Copolymer Microgels

P(NIPAM-GMA)CYS (1mg/mL) was incubated with citrate-GNP in a volume ratio of copolymer microgel to GNP of 1:5. Five incubations with addition of GNP followed by purification were performed for the formation of the nanocomposite. The solution appearance changed from the characteristic color of P(NIPAM-GMA) copolymer microgels (slightly opaque) to pink upon incubation with GNP. The nano-composite P(NIPAM-GMA)CYS-GNP was purified by centrifugation and characterized by UV-VIS measurements.

Second Polymerization with NIPAM: A mass of 2.5mg P(NIPAM-GMA)CYS-GNP was mixed with 100mg of NIPAM in 5mL of water to performed a second polymerization by precipitation polymerization. KPS (0.609mL of 0.015M) was added to initiate the reaction. The polymerization proceeded for 6 hours, at a stirring rate of 4rpm and a temperature of 70ºC. The resultant composite, P(NIPAM-GMA)CYS-GNP-PNIPAM was purified by centrifugation and characterized by DLS, TEM and UV-VIS.

Seeded-Mediated Growth of GNP: The seed-mediated growth of gold was achieved by adding 2.5mg of P(NIPAM-GMA)CYS-GNP-PNIPAM and 0.383mL of $HAuCl_4$ to 20mL of DI water in a scintillation vial. The solution was placed in an ice bath and stirred for 10 minutes. A volume of 0.625mL of hydroxylamine hydrochloride (reducing agent) was added to the solution while stirring. The composite solution was stirred for 40 minutes and purified by centrifugation (4 cycles). The composite P(NIPAM-GMA)CYS-GNP-PNIPAM-Au was characterized by DLS, TEM and spectroscopy.

3.3.2   Results and Discussions

Figure 24(A) shows the maximum absorbance peak of citrate-GNP was at 521nm. The DLS characterization (Figure 24(B)) shows that the mean size of the particles was ~6 nm in diameter. Combining both characterization results it was concluded that the synthesized citrate-GNP were monodisperse and colloidally stable in solution.

P(NIPAM-GMA)CYS copolymer microgels were opaque at room temperature. Figure 25 shows that turbidity increased slightly upon heating the solution above LCST. However, the opacity from the GMA core at room temperature reduces the magnitude of turbidity changes that is typically seen in microgels comprising of PNIPAM. DLS characterization of these amino-functionalized copolymer microgels (Figure 26) showed reversible volume transition and was similar to that observed in Figure 8 for P(NIPAM-GMA).

The results of P(NIPAM-GMA)CYS-GNP composite were promising in terms of loading and immobilization of GNP within the microgel network. Figure 27(A) shows the UV spectrum for the composite. The maximum absorbance peak was of ~523nm at room temperature, which is the characteristic of GNP. The composite showed a pink appearance at room temperature (Figure 27(B)) but the increase in the solution's turbidity upon heating was barely detected (not shown). Absorbance peak at ~40ºC was ~527nm. The reversible change in absorbance peaks at temperatures below and above LCST was indicative of immobilization and changes in interparticle distance of GNP within the system. The shift to longer wavelengths of absorbance peaks in the UV spectrum and optical behavior of the composite suggested that proximity of GNP in the composite was a function of the swelling/shrinking degree of the system. However, since this change

39

was very small, optical changes were not visible to the naked eye, presumably, due to the small size of GNP entrapped inside the microgel. TEM images (Figure 28) confirmed that the composite contained monodisperse and colloidally stable GNP. The images revealed that there was a high loading of GNP and that the particles were randomly dispersed throughout the copolymer microgel.

The samples wherein a second polymerization with NIPAM was performed exhibited an increase in mean diameter of approximately 250nm (Figure 29). This was probably caused by a high feed ratio of NIPAM to P(NIPAM-GMA)CYS-GNP composite during polymerization. The UV spectrum in Figure 30(A) showed that scattering from microgels dominated over the plasmon absorption of GNP at temperatures below and above LCST. The appearance of the solution, however, was not very different from that before the second polymerization (Figure 30(B)). TEM images in Figure 31 illustrate that GNP was retained in the composite after the second polymerization. The polymer matrix and complexion of GNP with amino groups were possibly stabilizing the GNP particles and prevented them from been affected by the polymerization temperature. However, slight aggregation of the GNP in the outer shell of the composites was observed. Unlike P(NIPAM-GMA)CYS-GNP, TEM images of P(NIPAM-GMA)CYS-GNP-PNIPAM also showed that the particle core-shell could not be distinguished anymore. It was concluded that a seeded growth of GNP by reduction of freshly added gold ions could overcome ambiguous color changes in the composite.

The purpose of growing the GNP by seeded growth was to enhance the optical properties of the composite as the interparticle distance changes upon varying the temperature of the microgel. The UV spectrum of the P(NIPAM-GMA)CYS-GNP-

PNIPAM-Au composite showed a GNP absorbance peak at 550nm that shifted to the right by ~40nm to 590nm when heated well above LCST (Figure 32(A)). Photographs in Figure 32(B) illustrate that the composite optical response due to the volume phase transition can be observed with the naked eye. The solutions appearance changed dramatically from red to purple suggesting decrease in GNP interparticle distance as microgels collapsed upon heating. The color changes of the composite were reversible after cooling down the solution.

TEM pictures confirmed the presence of larger GNP inside microgels (Figure 33). Figure 34 shows a plot of the wavelength of maximum absorption (λ_{max}) and the mean size of P(NIPAM-GMA)CYS-GNP-PNIPAM-Au composite as a function of temperature. An increase in λ_{max} was observed as temperature of the system increased. The value of λ_{max} increased continuously up to a temperature of 35ºC and then saturated. This trend was completely opposite to the trend in the mean size of the microgels and Figure 34 shows that the microgels collapsed with increasing temperature. The data suggests that beyond 35ºC, the interparticle distance of GNP cannot be reduced anymore. The temperature range where the mean size and wavelength curves cross can be used as an optimal condition for binding of metal ions in sensing schemes. According to the graph this conditions occur at or near 32ºC, which coincides, not surprisingly, with the transition temperature of PNIPAM.

From the experiment reported in this section it was concluded that optical properties and responses of thermally-responsive P(NIPAM-GMA)CYS-GNP composites can be enhanced by a combination of a higher amount of PNIPAM chains followed by seeded growth of the GNP inside the microgels. One of the drawbacks of this approach

was the need to perform many multiple steps to obtain the final composite. This makes

the preparation of the system to be complex and time consuming. Another limitation is

the lack of functional groups in the final composite for binding metal ions and for

exploiting any imprinting techniques.

3.4   Nanocomposites Based on PNIPAM/PAA-IPN Microgels

To develop an enhanced composite system through easier and faster steps, we

followed a strategy relying on interpenetrated networks of PNIPAM microgels and PAA

in combination with positively charged GNP. IPNs of PNIPAM and PAA, as seen in

Chapter 2, exhibited a thermal-behavior similar to PNIPAM microgels. PAA contains

COO^- groups that can potentially bind metal cations. However, for this composite system,

the COO^- groups can also be used to electrostatically stabilize GNP within the matrix of

the IPN. To achieve this, a cationic surfactant, cetyl-trimethylammonium bromide

(CTAB), was used. The nanocomposites were prepared by mixing PNIPAM/PAA-IPN-II

with CTAB coated GNP.

3.4.1   Experimental Section

Materials

Cetyl-trimethylammonium bromide (CTAB), and ascorbic acid were both

purchased from Sigma-Aldrich (WI).

Synthesis of Gold Nanoparticles Stabilized by CTAB

Citrate-GNP (~6nm) prepared and characterized as previously reported (see

section 3.3.2). A 0.1M solution of CTAB was prepared by heating it to 30ºC until

dissolving the surfactant. To replace the citrate ion, 63μL of 0.01M HAuCl$_4$ 500μL of

0.1M CTAB, and 12.5μL of a freshly prepared 0.1M ascorbic acid were added to the

scintillation vial containing 3 ml of citrate-GNP solution. The mixture was gently stirred

for 1 hour. The particles were characterized by DLS and UV-VIS.

Nanocomposite Based on PNIPAM/PAA-IPN Microgels

The thermo-responsive composites PNIPAM/PAA-GNP were prepared by mixing

250μL of 20mg/mL PNIPAM/PAA-IPN-II and 500μL of CTAB-GNP (1.017 x 10^{13}

particles) in a 1.5mL centrifuge tube. The solution was continuously stirred for six hours

using a vortex mixer. The product was purified by centrifugation and characterized by

UV-VIS spectroscopy and TEM.

3.4.2   Results and Discussions

DLS characterization of Citrate-GNP and CTAB-GNP particles is shown in

Figure 35. The mean size determined was ~6nm and 8nm, respectively. The UV-VIS of

Citrate-GNP, which is illustrated in Figure 36, shifted by 10nm to the higher wavelengths

after substituting its surface with CTAB.

The nanocomposite was easily prepared and redispersed in water after purification

by centrifugation. Figure 37 shows the UV spectrum for the composite at room

temperature and at a temperature above LCST. Upon comparison of Figure 36 and Figure

37, the absorbance peak at room temperature was observed at same wavelength of

CTAB-GNP. However, the scattering of PNIPAM/PAA IPN microgels dominated that of

CTAB-GNP in the composite at room temperature. When the composite was exposed to a

temperature above LCST the original absorbance peak at 522nm shifted by 29nm to the

higher wavelengths, which is indicative of a decrease in interparticle distance (Figure 37). However, a color change as in the case of P(NIPAM-GMA)CYS-GNP-PNIPAM-Au was not observed.

Since the mean size thermal-behavior of the IPN composite is enough to induce such a dramatic shift in the UV spectrum of GNP, there is no need for a second polymerization with NIPAM. Growing of GNP is an option but the presence of COOH could lead to nucleation in through out the system other than in the CTAB-GNP seed. This could result in polydispersity, aggregation and changes in the characteristic properties of GNP and the composite as a whole. Increase in the loading of GNP can be done easily by additional incubations of CTAB-GNP as performed for P(NIPAM-GMA)CYS-GNP. TEM of PNIPAM/PAA-IPN-GNP confirmed the presence of CTAB-GNP inside the matrix of the composite (Figure 38). The images show that the loading of GNP can be further optimized.
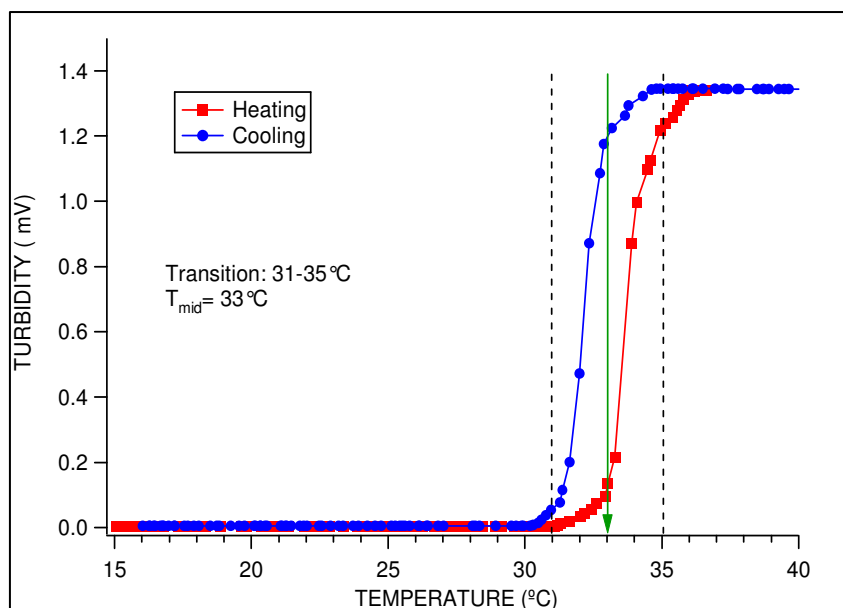
Figure 15: Turbidity data of PNIPAM-2%-Citrate-GNP.
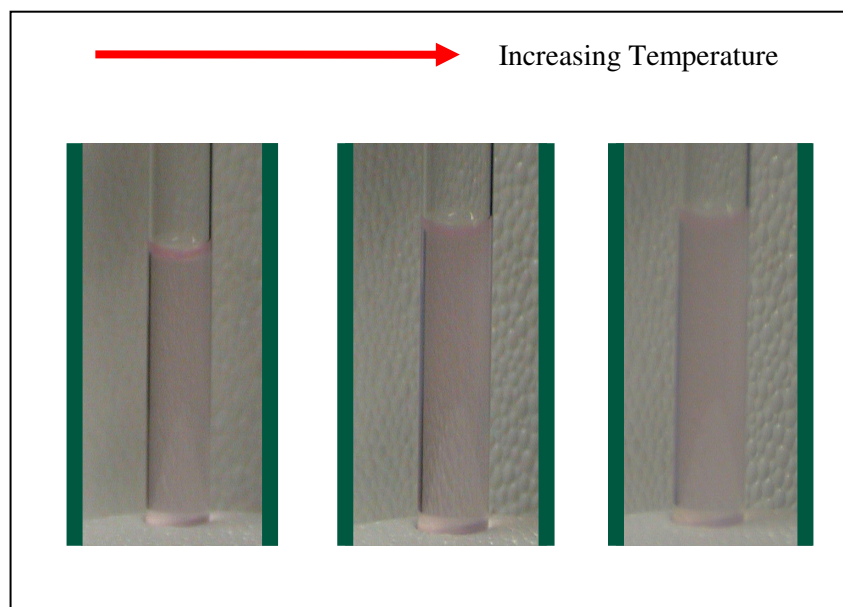
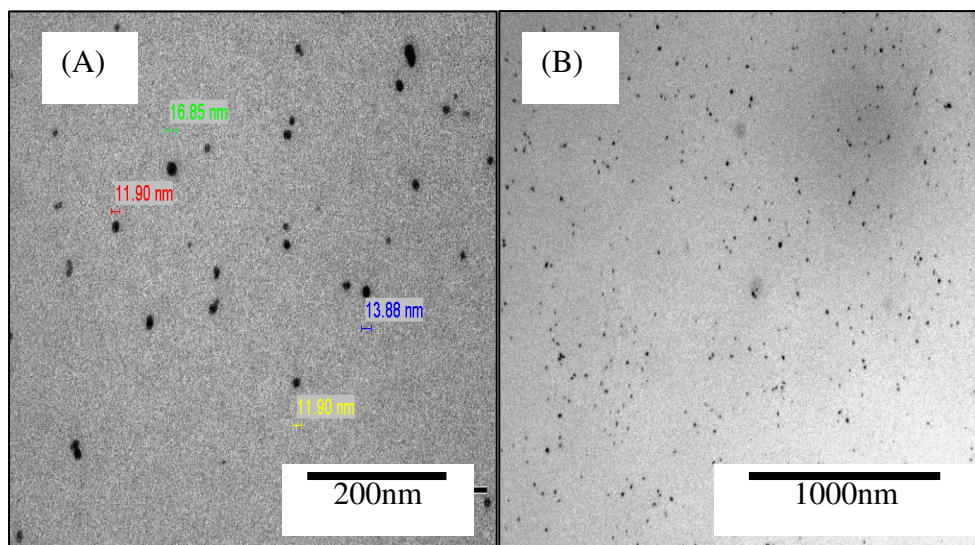**Figure 16: Changes in appearance of PNIPAM-2%-Citrate-GNP.**

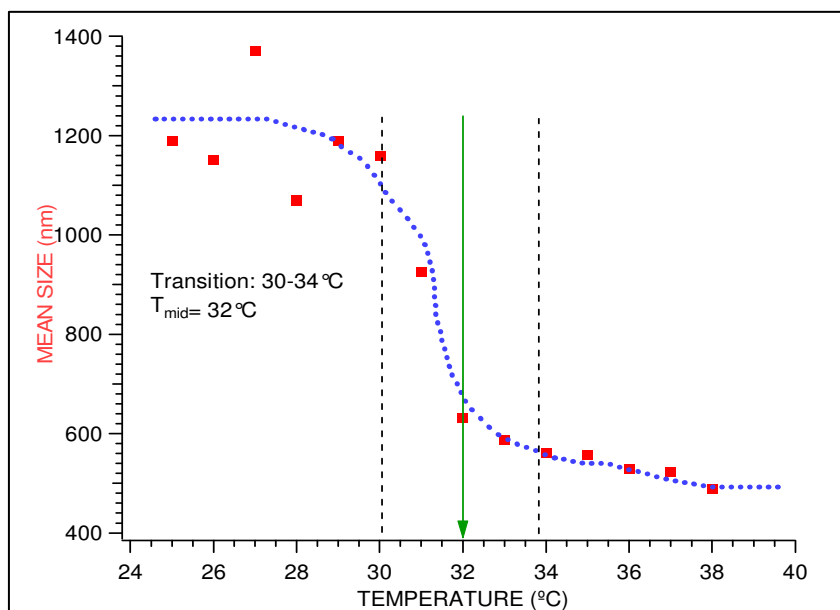**Figure 17: TEM of (A) Citrate-GNP; (B) PNIPAM-2%-Citrate-GNP.**

Transition: 30-34 ℃
T_{mid}= 32 ℃

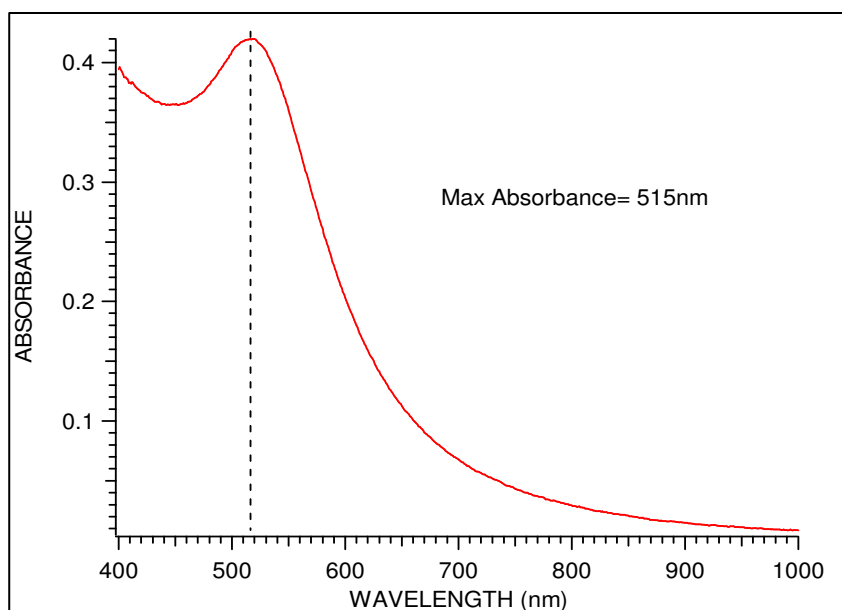**Figure 18: DLS of P(NIPAM-AA). Lines are drawn as a guide.**

Figure 19: UV-VIS of TOAB-GNP.
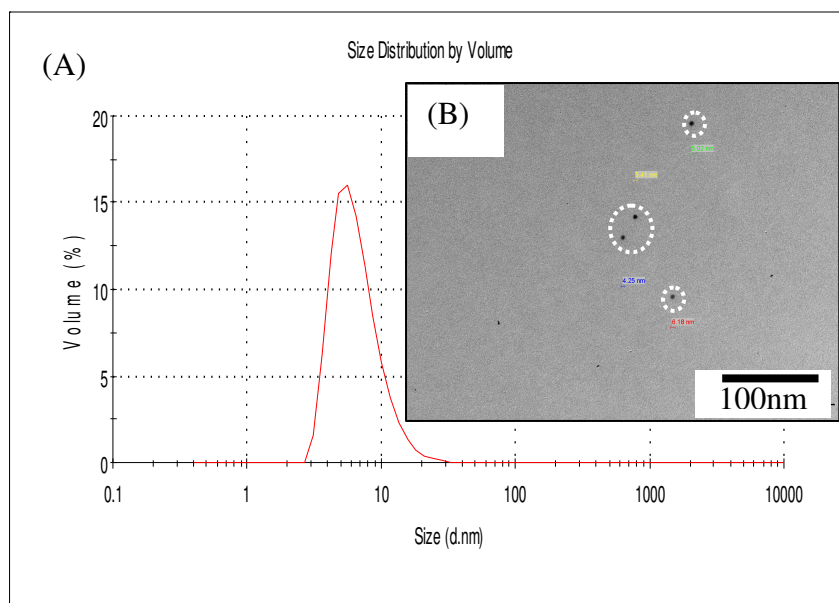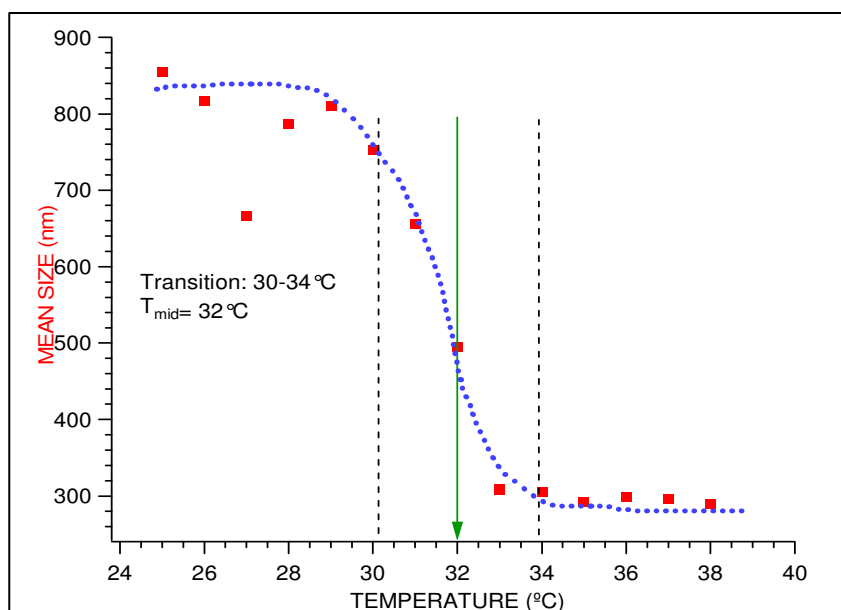

Figure 20: (A) DLS and (B) TEM of TOAB-GNP.

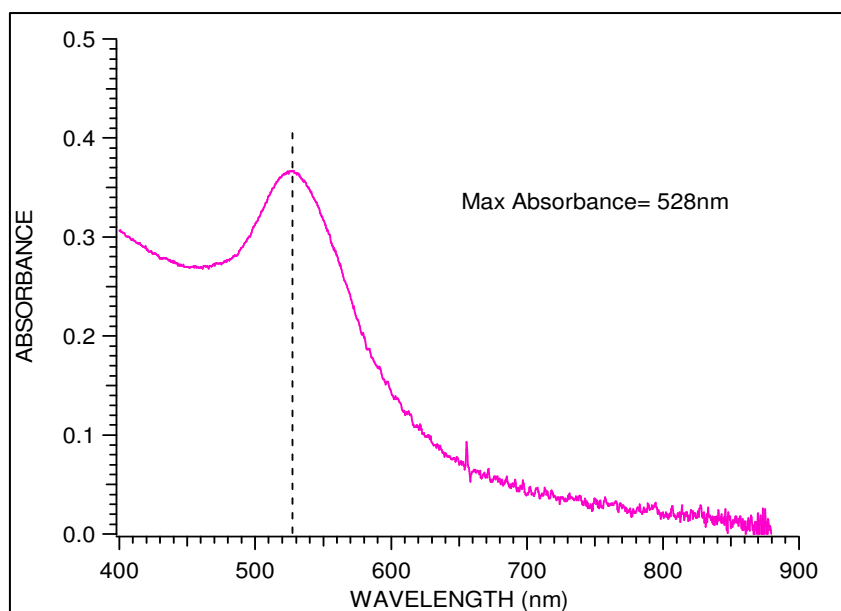**Figure 21: DLS of P(NIPAM-AA)DMAP-GNP. Lines are drawn as a guide.**

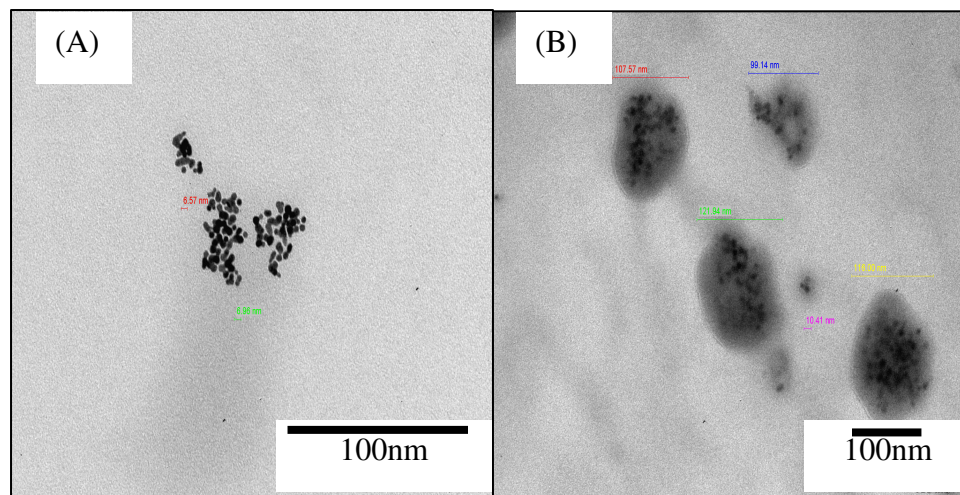**Figure 22: UV-VIS of P(NIPAM-AA)DMAP-GNP.**

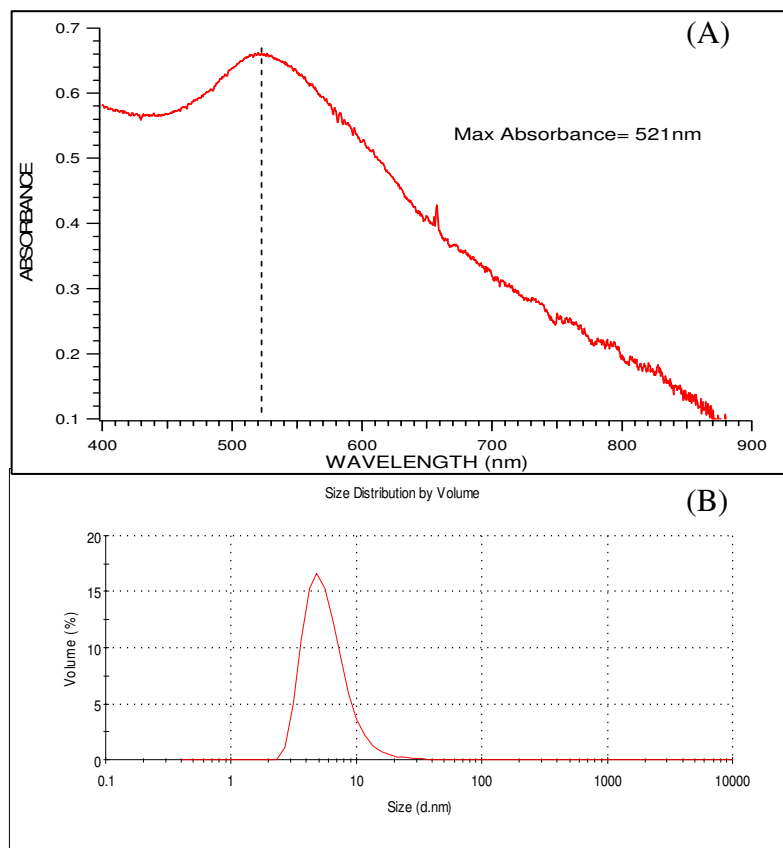**Figure 23: TEM of (A) DMAP-GNP; (B) P(NIPAM-AA)DMAP-GNP.**

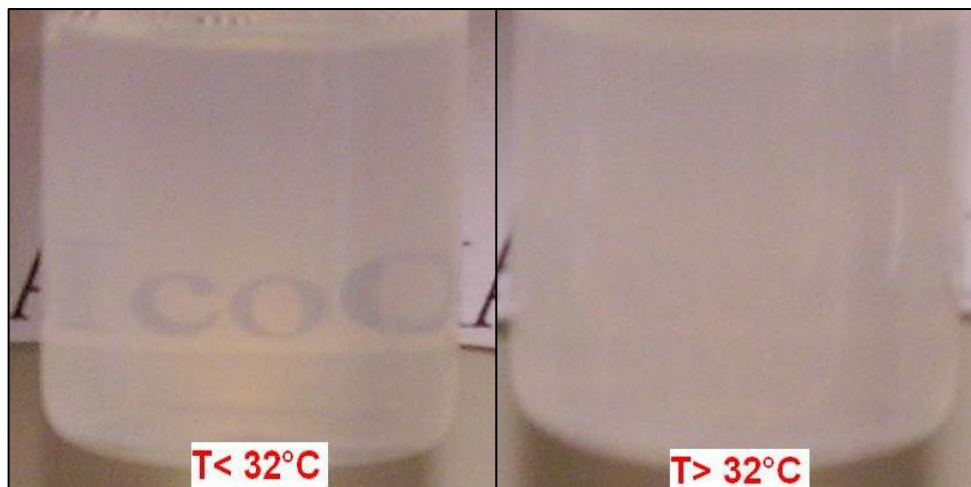**Figure 24: (A) UV-VIS and (B) DLS of Citrate-GNP.**

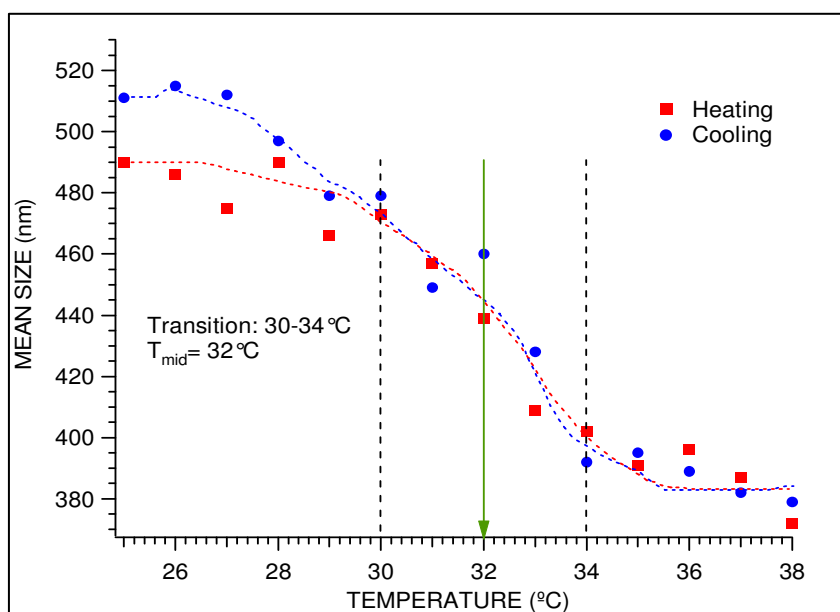**Figure 25: Appearance of P(NIPAM-GMA)CYS.**

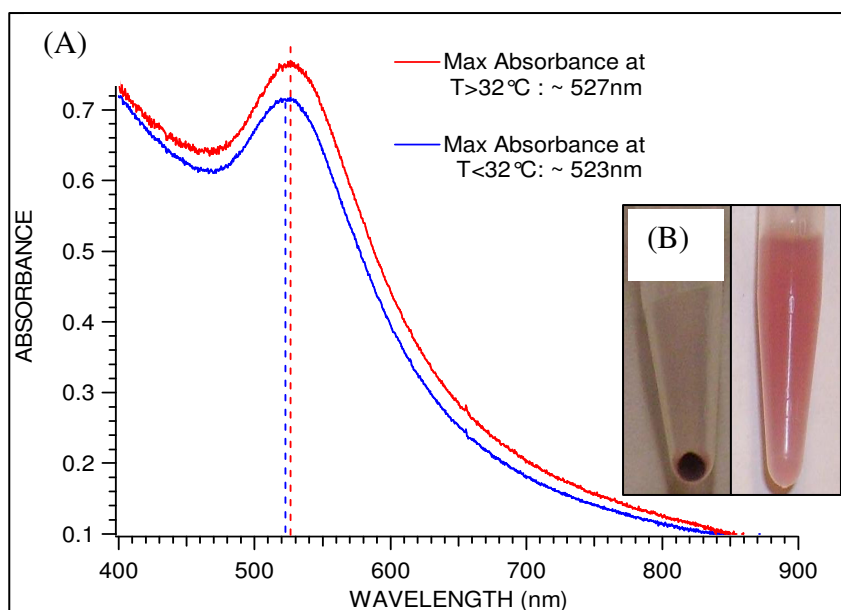**Figure 26: DLS of P(NIPAM-GMA)CYS. Lines are drawn as a guide.**

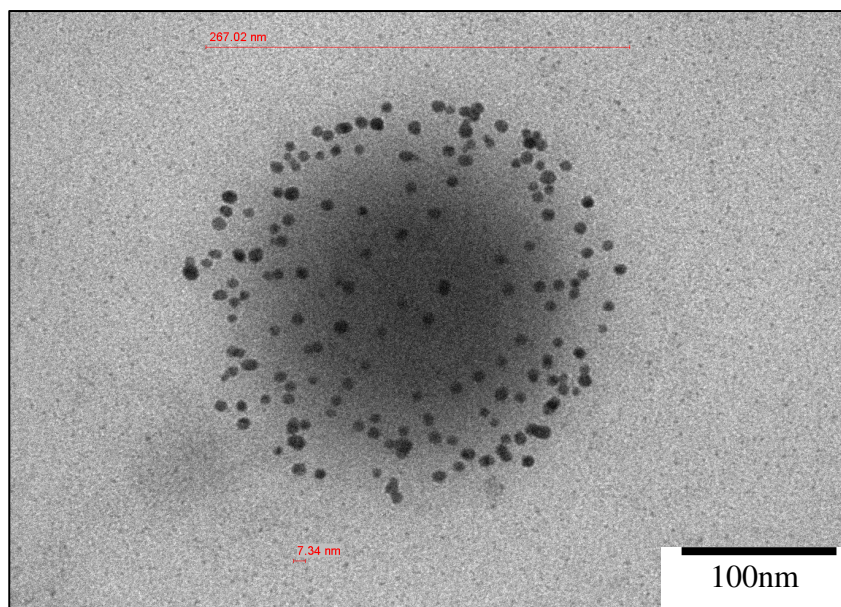**Figure 27: (A) UV-VIS and (B) Appearance of P(NIPAM-GMA)CYS-GNP.**

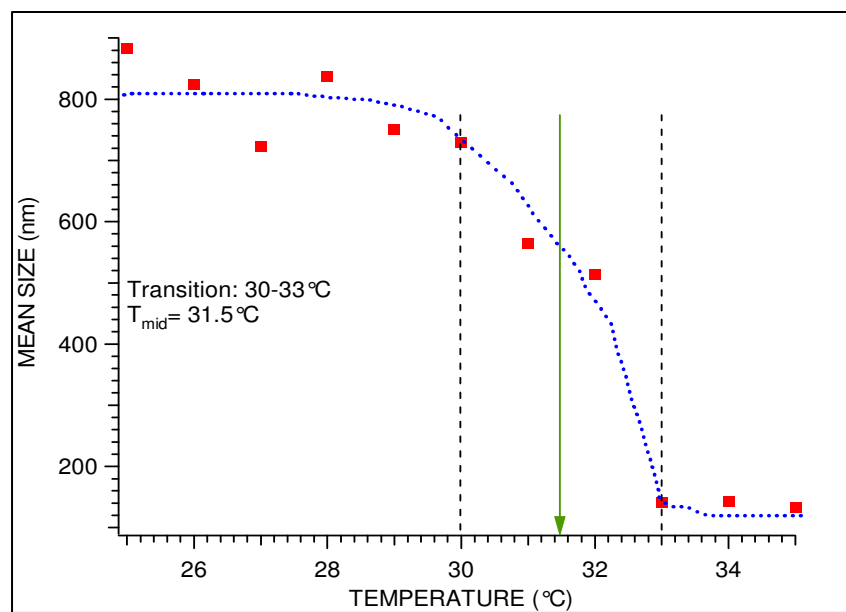**Figure 28: TEM of P(NIPAM-GMA)CYS-GNP.**

Figure 29: DLS of P(NIPAM-GMA)CYS-GNP-PNIPAM. Lines are drawn as a guide.
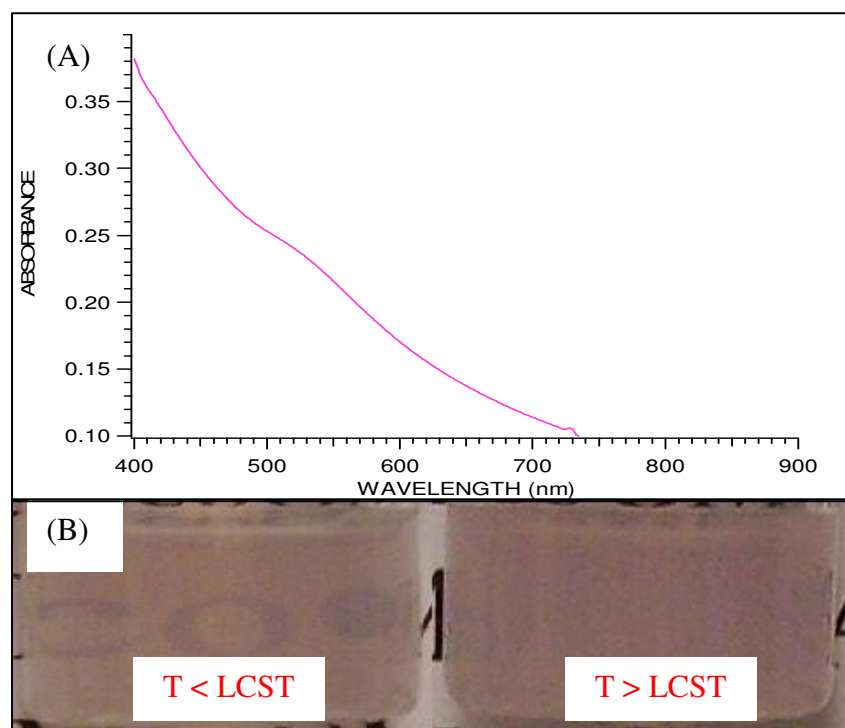
Figure 30: (A) UV-VIS and (B) Change in appearance of P(NIPAM-GMA)CYS-GNP-PNIPAM.
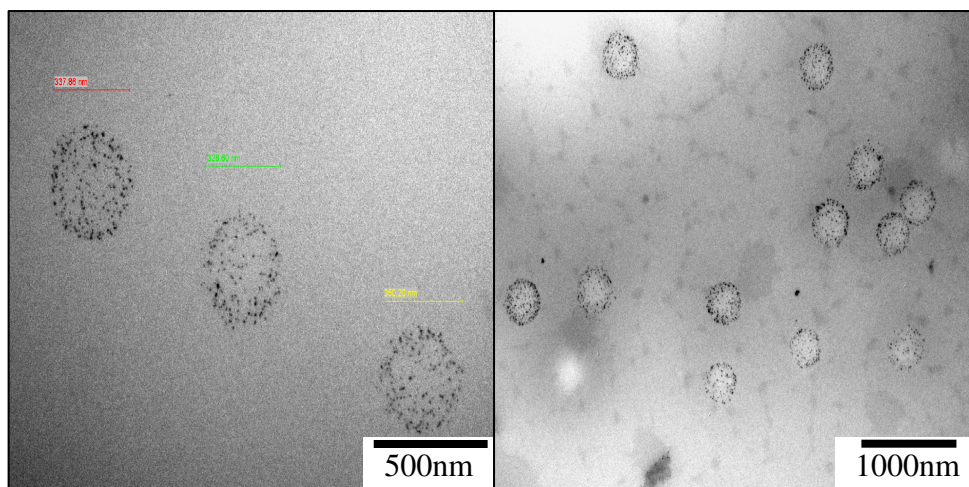
Figure 31: TEM of P(NIPAM-GMA)CYS-GNP-PNIPAM.
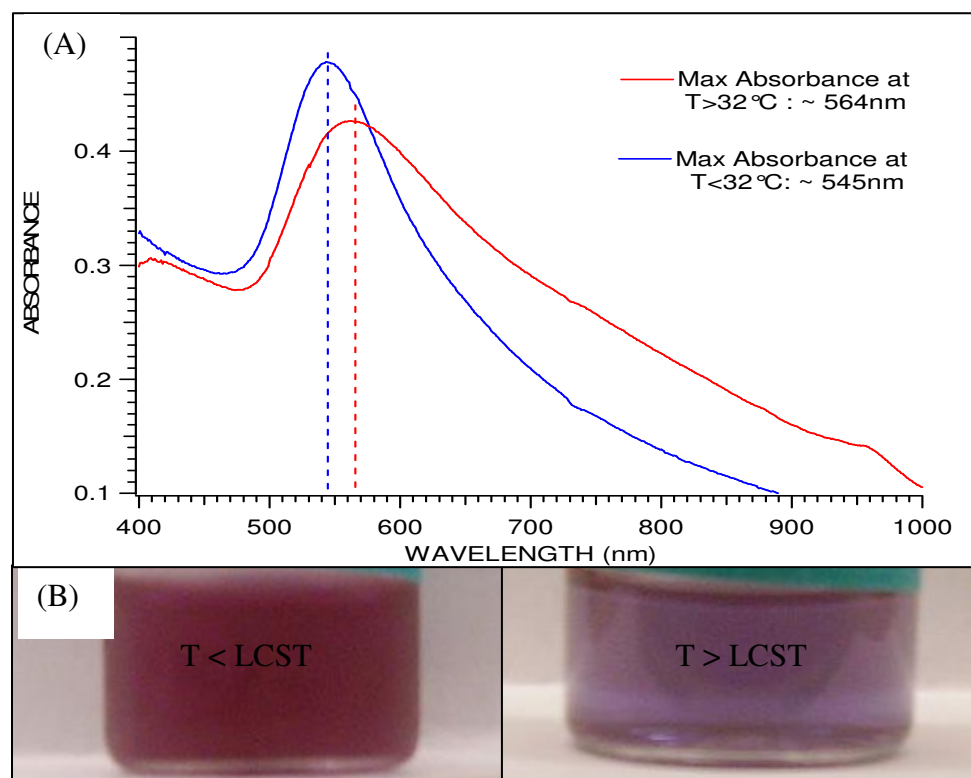
Figure 32: (A) UV-VIS and (B) Change in appearance of P(NIPAM-GMA)CYS-GNP-PNIPAM-AU.
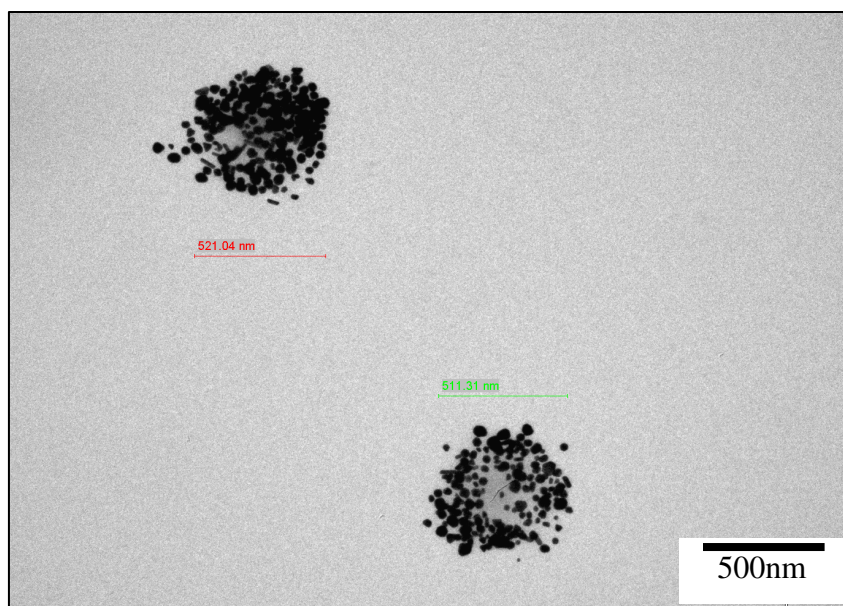
Figure 33: TEM of P(NIPAM-GMA)CYS-GNP-PNIPAM-AU.
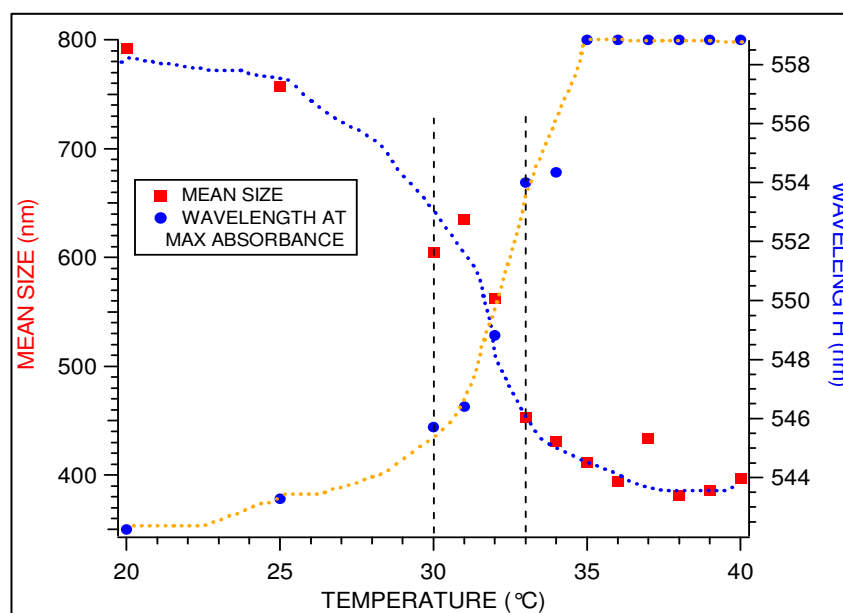
**Figure 34: Thermal relationship between wavelength at maximum absorbance and
mean size of P(NIPAM-GMA)CYS-GNP-PNIPAM-AU. Lines are drawn as a guide.**
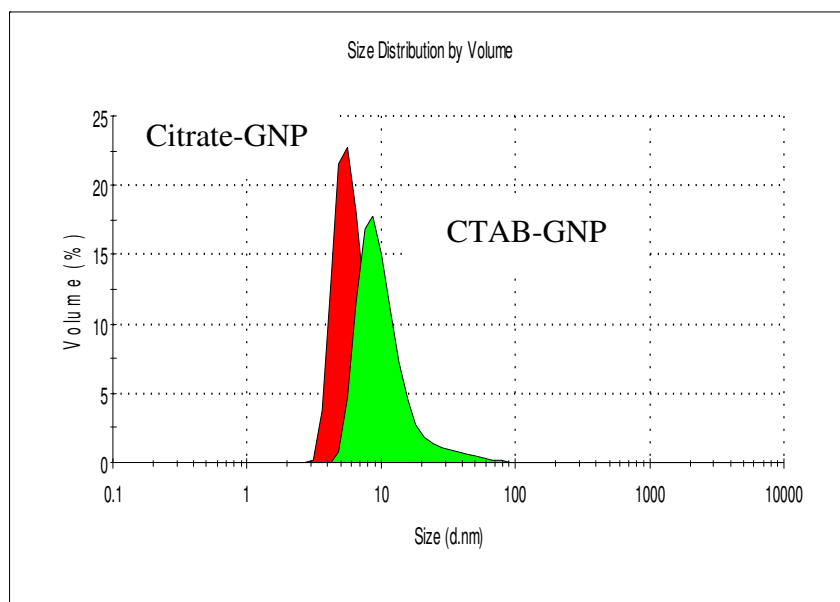
Figure 35: DLS of Citrate-GNP and CTAB-GNP.
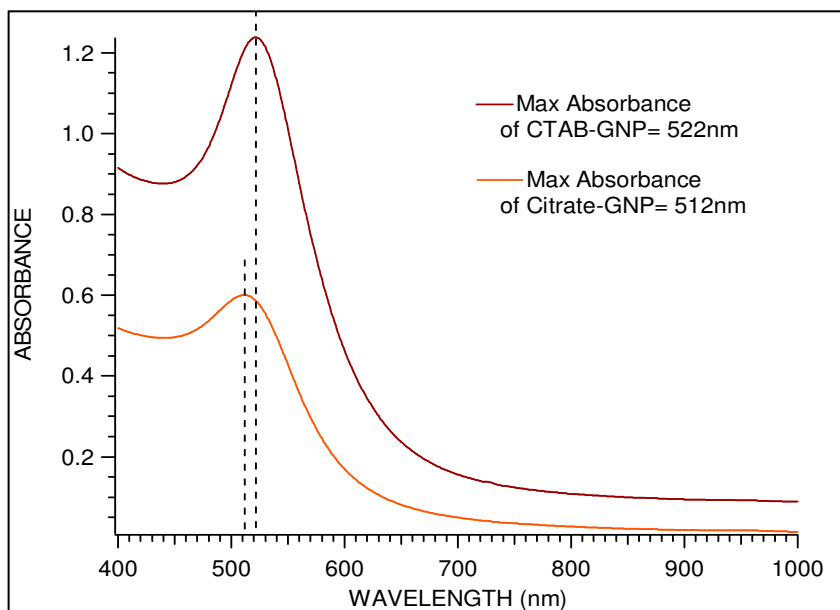
Figure 36: UV-VIS of Citrate-GNP and CTAB-GNP.
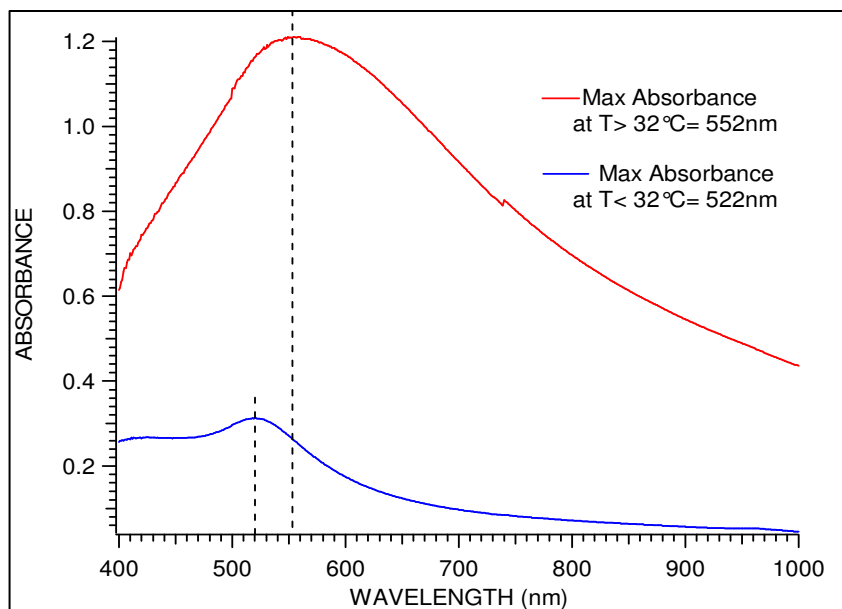
Figure 37: UV-VIS of PNIPAM/PAA-IPN-GNP.
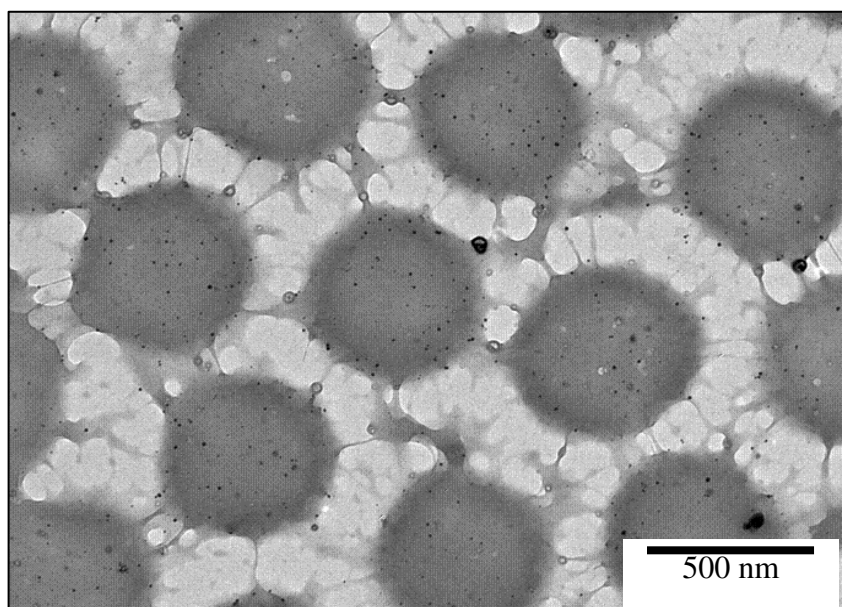
Figure 38: TEM of PNIPAM/PAA-IPN-GNP.

CHAPTER FOUR: MOLECULARLY IMPRINTED POLYMERS (MIP)

4.1 Molecularly Imprinted Polymers Based on PNIPAM/PAA IPN Microgels

One of the tasks in the thesis project was to study imprinted microgels for binding heavy metal ions such as copper. The thermo-responsive polymer selected was PNIPAM/PAA-IPN microgels because their polyelectrolyte units provide a large amount of binding sites for the metal ion. The preparation of the MIP was explored by performing a second polymerization on the microgels in presence of the target analyte at various cross-linking densities. The goal was to memorize the shape of the analyte, copper (Cu^{2+}) in this case, to make an MIP based on PNIPAM/PAA-IPN microgels that could selectively bind the target analyte. Since PNIPAM/PAA can respond reversibly to thermal stimuli, the recognition ability of the imprinted microgel could be controlled by temperature.

4.1.1 Experimental Section

Materials

2-methylsulfoxide (DMSO) was purchased from Sigma Aldrich (WI) and 4,4-azobis (4-cyanovaleric acid) was a sample from Wako Chemicals. Copper acetate (II) was purchased from Acros Chemicals (NJ).

Synthesis of MIPs Based on PNIPAM/PAA-IPN Microgels

The carboxylic acid sites in PNIPAM/PAA-IPN-II microgels were neutralized with 1M aqueous NaOH. A three-fold excess amount of 1.5M copper acetate (II) was added to the microgel solution relative to amount of PAA in the IPN. Mixing was continued for 24 hours to exchange the Na^+ with Cu^{2+}. Purification of PNIPAM/PAA-IPN-Cu^{2+} to remove the unbound Cu^{2+} consisted of dialysis for 1 day and 4 cycles of centrifugation at 8500 rpm for 30 minutes. The polymer was vacuum dried overnight at 30ºC.

For the second polymerization on PNIPAM/PAA-IPN-Cu^{2+} to imprint the target ion the solvent was changed to DMSO [8, 45, 52, 53]. Microgels can be redispersed in DMSO but they do not undergo volume phase changes in this solvent. After dispersing dried PNIPAM/PAA-IPN-Cu^{2+} in 1mL of DMSO and adding NIPAM and MBA according to values in Table 7, the reaction mixture was stirred and bubbled with N_2 for 30 minutes. The initiator solution in DMSO, 1mol% of ACVA, was also bubbled with N_2 for 30 minutes. The reaction mixture was heated to 60ºC, initiated by ACVA, and the reacted was allowed to proceed for 4 hours. The product was mixed with water and centrifuged 4 times to separate the microgels from DMSO. After removing the bound Cu^{2+} by adding several aliquots of 0.1M HCl, the product was rinsed several times with DI water and purified by centrifugation. Redispersion of the resultant precipitate in water was achieved by prolonged sonication and mixing with a vortex mixer. The imprinted polymer was tested using DLS.

Table 7: Formulation used for molecularly imprinted PNIPAM/PAA microgels.

SAMPLE	IPN (mg)	Cu^{2+} [1.5M] (ml)	NIPAM (mg)	MBA (mg)	DMSO (ml)
PNIPAM/PAA-MIP-4%	10	0.116	100	5	1
PNIPAM/PAA-MIP-7%	10	0.116	100	10	1
PNIPAM/PAA-MIP-10%	10	0.116	100	15	1

4.1.2 Results and Discussions

DLS characterization of PNIPAM/PAA-MIP cross-linked at 4, 7 and 10% is shown in Figures 39, 40, and 41, respectively. The mean size and volume phase transition of PNIPAM/PAA-MIP-4% were very similar to that observed for PNIPAM/PAA-IPN microgels. However, the mean size of PNIPAM/PAA-MIP-7% and PNIPAM/PAA-MIP-10% microgels decreased at swollen state by ~70 and ~100nm, respectively. The resultant mean size discrepancy for the MIPs cross-linked at 7 and 10% was attributed to the increase in cross-linking density inside the microgels and reduction in swelling.

Since our results showed that cross-linking took place within the PNIPAM/PAA-IPN, the next step was to determine if recognition sites for Cu^{2+} were formed. To accomplish this, the volume phase changes of 1mg of PNIPAM/PAA-MIP-10% in aqueous solution were investigated from 20-35ºC with different concentrations of Cu^{2+}. It was expected that the swelling degree of the MIP at various metal ion concentrations would reflect the occurrence of the templated sites. As the microgels shrink in response to temperature and the –COOH groups come in close proximity, we expected that the MIP would show a recognition for the Cu^{2+} ions and that this would be manifested in the size. Figure 42 shows a plot of PNIPAM/PAA-MIP-10% solution of 70μmoles of COOH groups and 0μmoles, 10μmoles, 15μmoles, and 20μmoles of Cu^{2+}. At concentrations of

10μmoles and 15μmoles the mean size of the MIP decreased and at 20μmoles of Cu^{2+} the mean size was that of the MIP containing no copper.

The imprinting of PNIPAM/PAA-IPN microgels by polymerization in DMSO decreased colloidal stability in water. This possibly influenced the preliminary data shown in Figure 42, which does not clearly show effects from the interaction with Cu^{2+}.
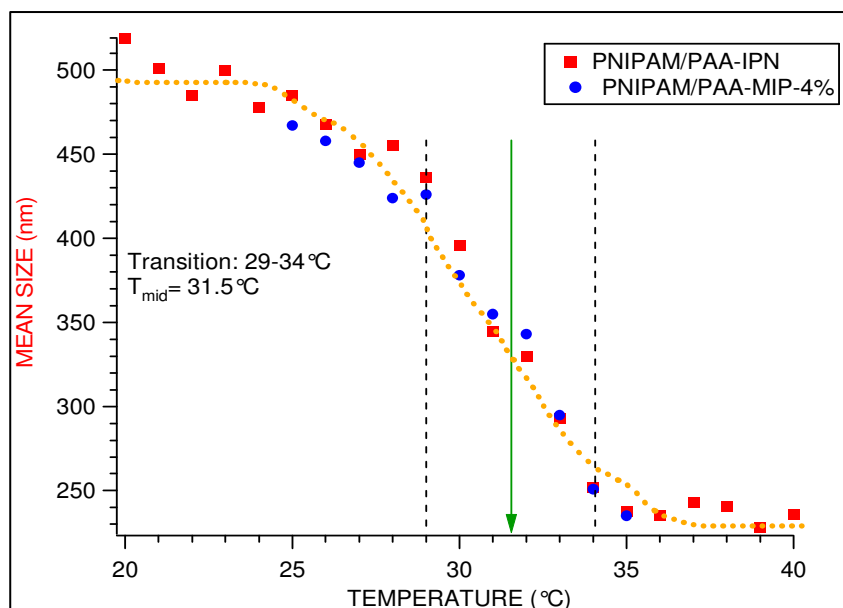
Figure 39: DLS of PNIPAM/PAA-MIP-4%. Lines are drawn as a guide.
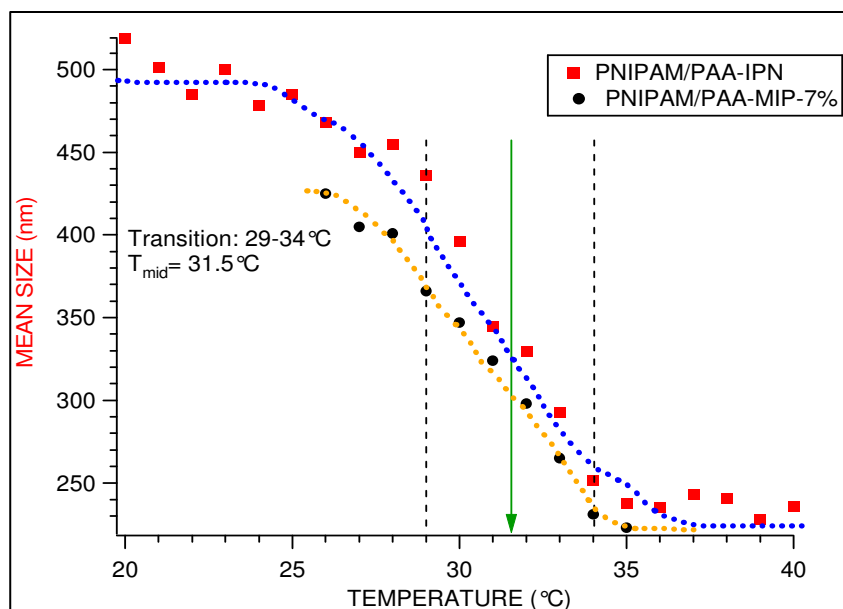

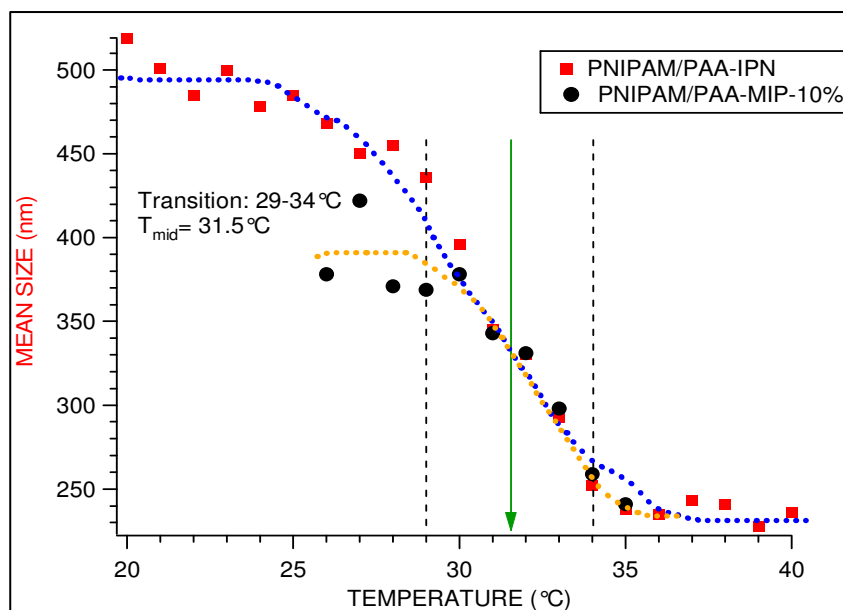**Figure 40: DLS of PNIPAM/PAA-MIP-7%. Lines are drawn as a guide.**

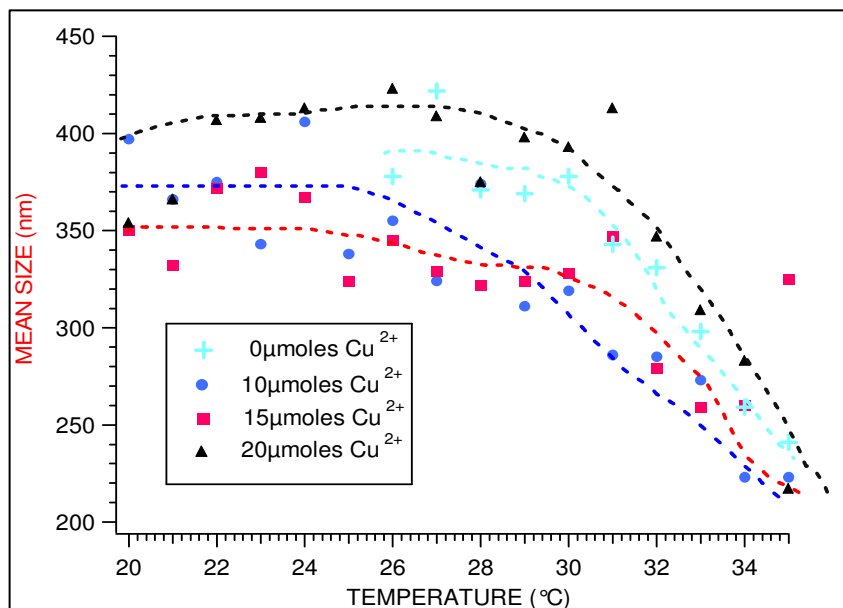**Figure 41: DLS of PNIPAM/PAA-MIP-10%. Lines are drawn as a guide.**

Figure 42: DLS of PNIPAM/PAA-MIP-10% at different copper ion concentrations. Lines are drawn as a guide.

CHAPTER FIVE: SUMMARY

In summary, the research described in this thesis has studied four distinct thermally-responsive materials: PNIPAM microgels, copolymeric microgels of P(NIPAM-AA), copolymeric microgels of P(NIPAM-GMA), and interpenetrated networks of PNIPAM/PAA. Both P(NIPAM-AA) and PNIPAM/PAA-IPN microgels provide polyelectrolyte units with carboxylic acid groups that can be used for the preparation of composites with GNP and also for the potential binding of metal cations. However, experiments described in Chapter 2 show that a higher concentration of carboxylic acid sites within the microgel network can be achieved by PNIPAM/PAA-IPN. Among the two methods to synthesize these IPN microgels, the one-step approach was found to be simpler. Copolymer microgels of P(NIPAM-GMA) were found to give functional groups that could be further used for the effective immobilization of GNP in the matrix of the microgels.

Among the strategies investigated for preparation of nanocomposites of thermally-responsive microgels and GNP, the most promising approach was found to be based on the PNIPAM/PAA-IPN microgels with carboxylic acid groups that were useful for the interaction with positively functionalized GNP coated with a cationic surfactant CTAB. In this system, the COOH groups can also serve as the useful sites for the binding of metal cations. An additional benefit of this approach as compared to composites described in Chapter 3, namely PNIPAM-2%-CitrateGNP, P(NIPAM-AA)DMAP-GNP,

and P(NIPAM-GMA)CYS-GNP-PNIPAM-AU, was that the system of PNIPAM/PAA-IPN-GNP was simple and quick to synthesize.

The experiments detailed in this thesis show that a lightly cross-linked sample, PNIPAM-2%-CitrateGNP, did not retain the GNP. This was possibly because of the lack of functional groups within the microgel network that can serve as driving force for the loading of GNP and as their stabilizer inside the matrix. A system that did possess functional groups from acrylic acid, P(NIPAM-AA)DMAP-GNP, failed to embed the GNP in the microgels because the GNP with a positively charged ligand such as DMAP had poor transferability of GNP from organic to aqueous medium and was difficult to reproduce. P(NIPAM-GMA)-GNP samples showed high loading of GNP within the microgel as well as promising thermal response of the composite and plasmon absorption shifts for the embedded GNP. However, the presence of GMA in the system limited the optical properties of the nanocomposite.

A preliminary study of imprinted microgels for binding heavy metal ions such as copper was performed using PNIPAM/PAA-IPN microgels. The imprinting of PNIPAM/PAA-IPN microgels required additional steps such as polymerization in an organic (DMSO) solvent, which caused subsequent problems of colloidal stability in water. We believe that this influenced the experiments that were done to test the selectivity of the MIP for Cu^{2+}. Therefore, results obtained from PNIPAM/PAA-IPN-MIP were not definitive. Future work on addressing these limitations is necessary.

REFERENCES

1. Committee on New Sensor Technologies: Materials and Applications, C. o. E. a. T. S., National Research Council, *Expanding the Vision of Sensor Materials*. ed.; The National Academies Press: 1995.

2. Davis, J. J.; Beer, P. D., Nanoparticles: Generation, Surface Functionalization, and Ion Sensing. *Dekker Encyclopedia of Nanoscience and Nanotechnology* 2004, 2477-2491.

3. Gerlach, G.; Guenther, M.; Sorber, J.; Suchaneck, G.; Arndt, K.-F.; Richter, A., Chemical and pH sensor based on the swelling behavior of hydrogels. *Sensors and Actuators, B: Chemical* 2005, B111-B112, 555-561.

4. WHITE, R. M., A Sensor Classification Scheme. *IEEE Transactions on Ultrasonic, Ferroelectrics, and Frequency Control* 1987, 34, 124-126.

5. Galaev, Y., 'Smart' polymers in biotechnology and medicine. *Russina Chemical Reviews* 1995, 64, 471-489.

6. Klabunde, K. J., *Nanoscale Materials In Chemistry*. ed.; John Wiley & Sons, Inc.: 2001.

7. Mingdi, Y.; Olof, R., *Moleculary Imprinted Materials: Science and Technology*. ed.; Marcel Dekker: New York, U.S.A., 2005.

8. Shea, K. J.; Yan, M.; Roberts, M. J., *Molecularly Imprinted Materials-Sensors and Other Devices*. ed.; Materials Research Society: Warrendale, Pennsylvania, 2002.

9. Nayak, S.; Lyon, L. A., Soft Nanotechnology with Soft Nanoparticles. *Angew. Chem. Int. Ed.* 2005, 44, 7686-7708.

10. Pelton, R. H.; Chibante, P., Preparation of aqueous latexes with N-isopropylacrylamide. *Colloids and Surfaces* 1986, 20, (3), 247-256.

11. Pelton, R., Unresolved Issues in the Preparation and Characterization of Thermoresponsive Microgels. *Macromol. Symp.* 2004, 207, 57-65.

12. Wu, C.; Zhou, S., Laser Light Scattering Study of the Phase Transition of Poly(N-isopropylacrylamide) in Water. 1. Single Chain. *Macromolecules* 1995, 28, 8381-8387.

13. Jones, C. D.; Lyon, L. A., Synthesis and Characterization of Multiresponsive Core-Shell Microgels. *Macromolecules* 2000, 33, (22), 8301-8306.

14. Benita, S.; Editor, *Microencapsulation: Methods and Industrial Applications. [In: Drugs Pharm. Sci., 1996; 73]*. ed.; 1996.

15. Das, M.; Sanson, N.; Fava, D.; Kumacheva, E., Microgels Loaded with Gold Nanorods: Photothermally Triggered Volume Transitions under Physiological Conditions. *Langmuir* 2007, 23, (1), 196-201.

16. Das, M.; Zhang, H.; Kumacheva, E., Microgels: Old Materials with New Applications. *Annual Review of Materials Research* 2006, 36, 117-142.

17. Das, M.; Mardyani, S.; Chan, W. C. W.; Kumacheva, E., Biofunctionalized pH-Responsive Microgels for Cancer Cell Targeting: Rational Design. *Adv. Mater.* 2006, 18, 80-83.

18. Xia, X.; Hu, Z., Synthesis and Light Scattering Study of Microgels with Interpenetrating Polymer Networks. *Langmuir* 2004, 20, (6), 2094-2098.

19. Yamashita, K.; Nishimura, T.; Nango, M., Preparation of IPN-type Stimuli-Responsive Heavy-Metal-Ion Adsorbent Gel. *Polym. Adv. Technol.* 2003, 14, 189-194.

20. Zhang, J.; Xu, S.; Kumacheva, E., Polymer Microgels: Reactors for Semiconductor, Metal, and Magnetic Nanoparticles. *J. Am. Chem. Soc.* 2004, 126, (25), 7908-7914.

21. Zhang, Y.; Wu, F.; Li, M.; Wang, E., pH switching on-off semi-IPN hydrogel based on crosslinked poly(acrylamide-co-acrylic acid) and linear polyallyamine. *Polymer* 2005, 46, (18), 7695-7700.

22. Bronstein, L. M., Polymer Colloids and Their Metallation. *Dekker Encyclopedia of Nanoscience and Nanotechnology* 2004, 2903-2915.

23. Brust, M.; Bethell, D.; Schriffrin, J.; Kiely, C. J., Novel gold-dithiol nano-networks with non-metallic electronic properties. *Adv. Mater.* 1995, 7, 795-7.

24. Demaille, C.; Brust, M.; Tsionsky, M.; Bard, A. J., Fabrication and Characterization of Self-Assembled Spherical Gold Ultramicroelectrodes. *Analytical Chemistry* 1997, 69, 2323-2328.

25. Guarise, C.; Pasquato, L.; Scrimin, P., Reversible Aggregation/Deaggregation of Gold Nanoparticles Induced by a Cleavable Dithiol Linker. *Langmuir* 2005, 21, 5537-5541.

26. Murphy, C. J.; Sau, T. K.; Gole, A. M.; Orendorff, C. J.; Gao, J.; Gou, L.; Hunyadi, S. E.; Li, T., Anisotropic Metal Nanoparticles: Synthesis, Assembly, and Optical Applications. *J. Phys. Chem. B.* 2005, 109, 13857-13870.

27. Rodríguez-Fernández, J.; Pérez-Juste, J.; Mulvaney, P.; Liz-Marzán, L. M., Spatially-Directed Oxidation of Gold Nanoparticles by Au(III)-CTAB Comploxes. *J. Phys. Chem. B.* 2005, 109, (30), 14257-14261.

28. Stevenson, P. C.; Hiller, J., *Discuss. Faraday Soc.* 1951, 11, 55-75.

29. Templeton, A. C.; Hostetler, M. J.; Warmoth, E. K.; Chen, S.; Hartshorn, C. M.; Krishnamurthy, M.; Vijay; Forbes, D. E. M.; Murray, R. W., Gateway Reactions to Diverse, Polyfunctional Monolayer-Protected Gold Clusters. *J. Am. Chem. Soc.* 1998, 120, 4845-4849.

30. Komiyama, M.; Takeuchi, T.; Mukawa, T.; Asanuma, H., *Molecular Imprinting: from Fundamentals to Applications.* ed.; Wiley-VCH: Rederal Republic of Germany, 2003.

31. Gao, H. Y., Wuli; Min, Ke; Zha, Liusheng; Wang, Changchun; Fu, Shoukuan., Thermosensitive poly(N-isopropylacrylamide) nanocapsules with controlled permeability. *Polymer* 2005, 46, 1087-1093.

32. Gao, J.; Frisken, B. J., Cross-Linker-Free N-Isopropylacrylamide Gel Nanospheres. *Langmuir* 2003, 19, (13), 5212-5216.

33. Kuang, M.; Wang, D.; Mohwald, H., Fabrication of Thermoresponsive Plasmonic Microspheres with Long-Term Stability from Hydrogel Spheres. *Adv. Funct. Mater.* 2005, 15, 1611-1616.

34. Kang, M.-S.; Gupta, V. K., Photochromic Cross-Links in Thermoresponsive Hydrogels of Poly(N-isopropylacrylamide): Enthalpic and Entropic Consequences on Swelling Behavior. *Journal of Physical Chemistry B* 2002, 106, (16), 4127-4132.

35. Varga, I.; Gilányi, T.; Mészáros, R.; Filipcsei, G.; Zrínyi, M., Effect of Cross-Link Density on the Internal Structure of Poly(N-isopropylacrylamide) Microgels. *J. Phys. Chem. B.* 2001, 105, 9071-9076.

36. *Zetasizer Nano Series User Manual.* ed.; Malvern Instruments Ltd.: England, 2005.

37.   Munk, P.; Aminabhavi, T. M., *Introduction to Macromolecular Science*. Second Edition ed.; John Wiley & Sons, Inc.: 2002.

38.   Serpe, M. J.; Lyon, L. A., Optical and Acoustics Studies of pH-Dependent Swelling in Microgel Thin Films. *Chem. Mater.* 2004, 16, (22), 4373-4380.

39.   Xu, S.; Zhang, J.; Paquet, C.; Lin, Y.; Kumacheva, E., From Hybrid Microgels to Photonic Crystals. *Adv. Funct. Mater.* 2003, 13, (6), 468-472.

40.   Suzuki, D.; Kawaguchi, H., Modification of Gold Nanoparticle Composite Nanostructures Using Thermoresponsive Core-Shell Particles as a Template. *Langmuir* 2005, 21, (18), 8175-8179.

41.   Suzuki, D.; Kawaguchi, H., Gold Nanoparticle Localization at the Core Surface by Using Thermosensitive Core-Shell Particles as a Template. *Langmuir* 2005, 21, (25), 12016-12024.

42.   Suzuki, D.; Kawaguchi, H., Hybrid Microgels with Reversibly Changeable Multiple Brilliant Color. *Langmuir* 2006, 22, 3818-3822.

43.   Jones, C. D.; Lyon, L. A., Dependence of Shell Thickness on Core Compression in Acrylic Acid Modified Poly(N-isopropylacrylamide) Core/Shell Microgels. *Langmuir* 2003, 19, (11), 4544-4547.

44.   Kanazawa, R.; Mori, K.; Tokuyama, H.; Sakohara, S., Preparation of Thermoresponsive Microgel Adsorbent for Quick Adsorption of Heavy Metal Ions by a Temperature Change. *Journal of Chemical Engineering of Japan* 2004, 37, (6), 804-807.

45.   Yamashita, K.; Nishimura, T.; Ohashi, K.; Ohkouchi, H.; Nango, M., Two-Step Imprinting Procedure of Inter-Penetrating Polymer Network-Type Stimuli-Responsive Hydrogel-Adsorbent. *Polymer Journal* 2003, 35, (7), 545-550.

46.   Link, S.; El-Sayed, M. A., Spectral Properties and Relaxation Dynamics of Surface Plasmon Electronic Oscillations in Gold and Silver Nano-dots and Nano-rods. *J. Phys. Chem. B.* 1999, 109, 8410.

47.   Li, G.; Wang, T.; Bhosale, S.; Zhang, Y.; Fuhrhop, J.-H., Completely Reversible Aggregation of Nanoparticles by Varying the pH. *Colloid Polymer Science* 2003, 281, 1099-1103.

48.   Pong, F. Y.; Lee, M. e.; Bell, J. R.; Flynn, N. T., Thermoresponsive Behavior of Poly(N-Isopropylacrylamide) Hydrogels Containing Gold Nanostructures. *Langmuir* 2006, 22, 3851-3857.

49.   Wang, C.; Flynn, N. T.; Langer, R., Controlled Structure and Properties of Thermoresponsive Nanoparticle-Hydrogel Composite. *Adv. Mater.* 2004, 16, (13), 1074-1079.

50.   Gandubert, V. J.; Lennox, R. B., Assessment of 4-(Dimethylamino)pyridine as a Capping Agent for Gold Nanoparticles. *Langmuir* 2005, 21, 6532-6539.

51.   Gittins, D. I.; Caruso, F., Biological and Physical Applications of Water-Based Metal Nanoparticles Synthesized in Organic Solutions. *Chem. Phys. Chem* 2002, 1, (3), 110-113.

52.   Matsui, J.; Akamatsu, K.; Hara, N.; Miyoshi, D.; Nawafune, H.; Tamaki, K.; Sugimoto, N., SPR Sensor Chip for Detection of Small Molecules Using Molecularly Imprinted Polymer with Embedded Gold Nanoparticles. *Analytical Chemistry* 2005, 77, (13), 4282-4285.

53.   Matsui, J.; Akamatsu, K.; Nishiguchi, S.; Miyoshi, D.; Nawafune, H.; Tamaki, K.; Sugimoto, N., Composite of Au Nanoparticles and Molecularly Imprinted Polymer as a Sensing Material. *Analytical Chemistry* 2004, 76, (5), 1310-1314.